Rational Drive for School Segregation in a Model of Learning

Peter Galbács

September 22, 2026

Abstract

We develop a dynamic two-sector heterogenous-agent model of formal schooling in which each student's human-capital accumulation depends on study time, previously acquired knowledge, and a positive peer externality *à la* Lucas (1988). In our benchmark, families perfectly observe prospective classmates' innate learning efficiencies. We derive closed-form steady-state solutions and prove saddle-path stability for both decentralized equilibrium and the social-planner optimum. Our analysis reveals an asymmetric sorting motive: high-ability households strongly prefer clustering with similar peers, while low-ability households have weaker segregation incentives. By relocating knowledge spillovers from production into the schooling sector, the model isolates a pure drive to segregate by learning capacity and offers a novel mechanism for socioeconomic clustering in schools. We conclude by outlining the benchmark's abstractions—perfect foresight, no search frictions, omitted calibration—and suggesting extensions to incorporate informational noise and policy analysis.

JEL codes: I20, I24, J24, C61
Keywords: human capital accumulation, optimal control, segregation, peer effects, externalities

1 Introduction

Lucas (1988) introduced knowledge spillovers in production as the engine of endogenous growth, framing knowledge as a factor whose productivity depends on the average knowledge of society. Empirical work reveals a parallel phenomenon in classrooms—peer effects—where classmates' knowledge (or simply the quality of the learning environment) boosts the efficiency of individual human-capital accumulation. Anticipating these peer-driven gains, families strategically choose schools for their children, helping to explain why classrooms often cluster along socioeconomic lines.

Extensive research documents the adverse consequences of school segregation on student outcomes. Schools sorted by race or income typically suffer from inadequate funding, fewer experienced teachers, and limited instructional resources—conditions that depress test scores and long-run prospects (Borman et al., 2003; Weathers and Sosina, 2022). Recent studies also link segregation to setbacks in cognitive development and psychological well-being among disadvantaged students (Gutierrez et al., 2024; Peterson et al., 2021). In this account, segregation stands as the root cause of material and institutional barriers that erode learning.

Since the Coleman Report (Coleman et al., 1966), a related strand of literature has highlighted peer effects as a key channel through which students influence one another's outcomes (Sacerdote, 2011). Classmates' socioeconomic backgrounds and achievement levels shape individual test scores, motivation, and long-term success. Segregation magnifies these dynamics by grouping students with similar challenges, which can limit the academic stimulation and support found in more integrated settings. Empirical and theoretical work shows that expectations about peer quality drive families' school-choice decisions, reinforcing segregation as households seek the most advantageous learning environment (Manski, 1993; Epple and Romano, 1998; Orfield and Lee, 2007). From this perspective, socioeconomic segregation stems not only from disparities in funding and institutional rules but also from families' rational responses to anticipated peer effects.

In this paper, we isolate why rational households desire to self-segregate by learning ability, without modeling segregation's full emergence via search or matching. We embed peer effects into a two-sector Uzawa–Lucas framework, relocating Lucas's (1988) externality from production to the learning process. Under our benchmark assumption, families perfectly observe prospective classmates' innate learning efficiencies—a clean setup that yields closed-form steady states and transparent comparative statics. In Sector 1, human-capital accumulation is governed by a learning function that takes study time, previously acquired knowledge, and a positive peer externality as inputs. Sector 2 then translates accumulated human capital into utility through a standard consumption–leisure trade-off.

We present this model as a positive, mechanism-focused benchmark—while abstracting from informational noise in peer-ability signals, schooling-market search frictions or matching dynamics, on-the-job and familial human-capital externalities, quantitative calibration of parameters, and any normative or policy counterfactuals. Each of these could attenuate but is unlikely to overturn the core peer-sorting motive, and so we leave them for future extensions.

Anticipating that high-ability peers accelerate learning while lower-ability peers impose a drag, rational households tend to prioritize the school environment that maximizes their child's expected skill trajectory. High-efficiency families are therefore encouraged to cluster

together to capture positive peer gains, whereas low-efficiency families have little incentive to forgo integration as they benefit from mixing with stronger learners. This asymmetry in the desire to segregate—the strong sorting motive of high-ability households versus the weaker motive of low-ability ones—echoes the insights of Lucas and Moll (2014) on optimal learning environments and complements the early-life skill-formation literature (Cunha et al., 2010; Heckman and Masterov, 2007; Neal, 2018).

The paper unfolds as follows. In Section 2, we introduce a discrete-time overlapping-generations framework in which human-capital accumulation is driven by the prospect of future income; learning depends on previously acquired knowledge and the time each child devotes to study. Section 3 reformulates this setup in continuous time, constructs the representative household's Hamiltonian, and derives the existence and uniqueness conditions for the isolated learner's optimal control problem. Section 4 examines the stability of that optimum, while Section 5 fully characterizes the optimal time-allocation path for both the decentralized household and the social planner.

Building on this benchmark, Section 6 embeds a positive peer externality into the learning function, solves for both equilibrium and planner allocations, and shows how they diverge once classmates' abilities matter. To trace those dynamics back to the no-externality case, Section 7 applies the comparative-dynamics methods of Oniki (1973) and Caputo (1990a). Finally, Section 8 reflects on our core insights, aligns them with empirical patterns of school clustering, and flags avenues for future work.

To ensure full computational reproducibility, the complete Python package containing the replication files and simulation codes is publicly available on Zenodo (Galbács, 2026).

2 An overlapping generations model

In a family, each generation lives for two periods, so after being young it becomes old. At any time t, two generations—young and old—live simultaneously. In the first period of her life, the individual learns at school to accumulate human capital that she uses in the second part of her life when working. As a capital transfer from the previous generation, the member of the young generation living at time t (called the member of generation t when young) enters the school system with a knowledge level h_t^α with $0 < \alpha < 1$.

The human capital of the old generation living at time t (the member of generation $t-1$ when old) is h_t, so the parameter α determines the fraction of human capital transferred from the old to the young that the young generation uses to learn new skills. It must hold that $h_t^\alpha < h_t$ for all t, as the young generation cannot possess a higher capital level when entering the school system than their parents do. With $0 < \alpha < 1$, this implies $h_0 > 1$, so there is a minimum knowledge requirement for a family to enter school for the first time. This assumption captures the fact that children are supposed to have some skills and knowledge before starting formal education. This lower bound $h_0 > 1$ will be reinforced further in subsequent sections.

Depending on this capital transfer, a member of generation t when young realizes utility according to a strictly increasing and strictly concave school-performance function. For simplicity, this function is assumed to be

$$\ln(h_t^{\alpha}) = \alpha \ln(h_t).$$

Human-capital accumulation is described with a learning function

$$h_{t+1} = g(h_t, u_t),$$

according to which learning requires knowledge h_t and time u_t. For the young individual living in t, time investment is the decision variable, with $u_t \in [0, 1]$. Time investment is foregone leisure, so u_t is not included in the time someone spends learning at school. Accordingly, $u_t = 0$ means that time investment in learning is minimal and constrained to school activities. The function g is time-invariant, so the same learning capabilities characterize the whole dynasty.

Time investment is fraught with costs described by a strictly increasing and strictly convex cost function. For simplicity, a quadratic function $-Cu_t^2$ is assumed to describe the disutility of learning, with cost parameter $C > 0$. The higher C is, the higher the disutility (or equivalently, the lower the utility) realized from the same ratio of time.

Learning has a twofold purpose. Since in the second period of her life the individual works, her decision on time investment u_t partly depends on the present value of the expected return on human capital. This expected value is described with a strictly increasing and strictly concave function. For simplicity, this function is assumed to take the form

$$\beta B \ln(h_{t+1}),$$

in which $\beta > 0$ is the one-period discount factor and $B > 0$ is a parameter proportional to the value of the income stream generated by the human capital h_{t+1} accumulated for the second part of her life.

A young individual also considers the expected utility of her later child, given as $\beta U_{t+1}^*(h_{t+1})$, which is the time-t value of the maximum attainable utility from a given level of human capital owned in the second period of life, from which she transfers a fraction h_{t+1}^{α}. In other words, the young individual living in t deciding on u_t (hence h_{t+1}) also takes into account how much utility the next generation can realize from any given h_{t+1}, as her utility directly depends on her child's utility.

Therefore, assuming $h_1 = g(h_0, u_0)$, the problem of the decision maker in time 0 is

$$U_0^*(h_0) = \max_{u_0 \in [0,1]} \left\{ \alpha \ln(h_0) - Cu_0^2 + \beta B \ln(h_1) + \beta U_1^*(h_1) \right\}, \tag{2.1}$$

as the member of generation 1 when young makes her investment decision u_1 in the next period, $t = 1$, when living simultaneously with the individual who made her decision in time 0. The capital transfer h_0^{α} is wholly predetermined in the time-zero problem and comes from the currently living old member of generation -1.

The optimum levels of u_0 and h_1, given h_0, also depend on $U_1^*(h_1)$, so the member of generation 0 when young must also consider the problem of what utility her optimizing child will attain from any feasible h_1. Therefore, her problem widens and takes the form

$$\begin{aligned} U_0^*(h_0) = \max_{u_0, u_1 \in [0,1]} \Big\{ & \alpha \ln(h_0) - Cu_0^2 + \beta B \ln(h_1) \\ & + \beta \big[\alpha \ln(h_1) - Cu_1^2 + \beta B \ln(h_2) + \beta U_2^*(h_2) \big] \Big\}. \end{aligned} \tag{2.2}$$

Expanding the brackets yields

$$\begin{aligned} U_0^*(h_0) = \max_{u_0,u_1\in[0,1]} \Big\{ & \alpha \ln(h_0) - Cu_0^2 + \beta B \ln(h_1) \\ & + \beta\alpha \ln(h_1) - \beta C u_1^2 \\ & + \beta^2 B \ln(h_2) + \beta^2 U_2^*(h_2) \Big\}. \end{aligned} \tag{2.3}$$

subject to the law of motion

$$h_{t+1} = g(h_t, u_t).$$

Continuing this pattern, the sequential form becomes

$$\begin{aligned} U_0^*(h_0) = \max_{\{u_t\}_{t=0}^{\infty}} \Big\{ & \alpha \ln(h_0) - Cu_0^2 \\ & + \beta B \ln(h_1) + \beta\alpha \ln(h_1) - \beta C u_1^2 \\ & + \beta^2 B \ln(h_2) + \beta^2\alpha \ln(h_2) - \beta^2 C u_2^2 \\ & + \beta^3 B \ln(h_3) + \beta^3\alpha \ln(h_3) - \beta^3 C u_3^2 \\ & + \beta^4 B \ln(h_4) + \cdots \Big\}. \end{aligned} \tag{2.4}$$

The agent has control of u_0 (hence h_1) only, so all subsequent generations make their own decisions. Her child thus needs to find the optimal u_1 (hence h_2) given h_1, but this decision is the same as she expected her child to make from the h_1 she optimally determined for herself. When deciding on u_0 (hence h_1), she therefore foresaw her child's decision on u_1 (hence h_2), and so on for all future generations. Thus, the whole dynasty makes the same decisions as the member of generation 0 when young. We can therefore solve the overlapping-generations problem as the problem of an infinitely living representative agent, in line with Barro (1974).

The problem and its optimal solution do not change when a constant term is added to the objective function or when the objective function is scaled by a positive constant.[1] Accordingly, we can add $B\ln(h_0)$ and then multiply the augmented objective function by $1/(B+\alpha) > 0$, which yields

[1] (Bertsekas, 1976, p. 5) lays down the principle that an affine transformation of a payoff function that preserves the orderings of alternative policies yields the same solution. Likewise, if an optimal solution is regarded as an element of a sequence space such as $\{u_t\}_{t=0}^{\infty} \in l_\infty$, then the return function G is a functional on this space. If there is some program u^* such that $G(u) < G(u^*)$ where $G(u^*) = \sup\{G(x) : u \in l_\infty\}$ for any feasible program u, then with $a, b \in \mathbb{R}$ and $a > 0$ it holds that $aG(u) + b < aG(u^*) + b$ that can also be written as $\tilde{G}(u) < \tilde{G}(u^*)$, so the same solution emerges before and after the linear transformation of the payoff function.

$$
\begin{aligned}
U_0^*(h_0) = \max_{\{u_t\}_{t=0}^{\infty}} \Big\{ & \ln(h_0) - \frac{C}{B+\alpha} u_0^2 \\
& + \beta \ln(h_1) - \beta \frac{C}{B+\alpha} u_1^2 \\
& + \beta^2 \ln(h_2) - \beta^2 \frac{C}{B+\alpha} u_2^2 \\
& + \beta^3 \ln(h_3) - \beta^3 \frac{C}{B+\alpha} u_3^2 + \cdots \Big\}.
\end{aligned} \tag{2.5}
$$

This is equivalent to

$$
\max_{\{u_t\}} \sum_{t=0}^{\infty} \beta^t \left[\ln(h_t) - \frac{c}{2} u_t^2 \right], \tag{2.6}
$$

subject to

$$
h_{t+1} = g(h_t, u_t),
$$

where

$$
\frac{C}{B+\alpha} \equiv \frac{c}{2} > 0.
$$

In what follows, we solve the continuous-time version of eq. (2.6) with different specifications of the learning function g. The dynamic problem embedded in eq. (2.6) is to find an optimal path for the capital stock, the benefits of which can only be realized at the price of some disutility. Tomorrow's returns can only be increased by sacrificing some returns today.

3 An infinitely living representative agent in continuous time

The member of generation 0 when young is assumed to use human capital h_0^{α} with diminishing marginal product and time investment $u_0 \in [0, 1]$ in learning. Human capital h_{t+1} consists of two parts. The first part comes from learning with time investment and the use of the knowledge transfer, and arises as a stock containing only new skills not inherited from the previous generation. This part is

$$
A(h_t^{\alpha})^{\zeta} u_t,
$$

in which $0 < \zeta < 1$ describes the diminishing marginal productivity of human capital in learning, and $A > 0$. The other part comes from inherited knowledge subject to the depreciation of human capital from one generation to the next. If $\delta > 0$ is the depreciation rate determining how skills and knowledge lose their relevance from one generation to the next, then this part is simply $(1-\delta)h_t$. This component is acquired during school hours and requires no additional private time investment.

Therefore, the learning function g takes the form

$$h_{t+1} = A(h_t^{\alpha})^{\zeta} u_t + (1-\delta)h_t, \tag{3.1}$$

which implies

$$h_{t+1} - h_t = A(h_t^{\alpha})^{\zeta} u_t - \delta h_t. \tag{3.2}$$

Equation (3.2) is a discrete-time version of the learning function in Lucas (1988, eq. (13)), which is linear in time investment but exhibits diminishing marginal product of human capital. When $u_t = 0$, we have $h_{t+1} = (1-\delta)h_t$, so human capital in the next period equals the relevant part of the stock of knowledge remaining from the current period with no new knowledge added.

The learning function in (3.2) remains compatible with Lucas's idea of continuous technological progress even if it may imply (and, as we shall see, it does imply) a stable optimum stock of knowledge. At this stable level, a fraction of human capital disappears due to depreciation and is replaced with new and previously unpossessed knowledge. Therefore, knowledge and technology can continuously improve even though the stock of knowledge of each subsequent generation approaches a constant level.[2]

Diminishing marginal product of knowledge stems from the restriction on ζ. Parameter A governs the productivity of time and knowledge as factors of production in knowledge creation and describes what growth rate is achievable from unit capital and unit time investment. Note that (3.2) can be rewritten using the fact that

$$(h_t^{\alpha})^{\zeta} \equiv h_t^{\eta},$$

in which $0 < \eta < 1$ follows from the restrictions on α and ζ. Thus, the learning function becomes

$$h_{t+1} - h_t = Ah_t^{\eta} u_t - \delta h_t, \tag{3.3}$$

as the sequence $\{h_t\}_{t=0}^{\infty}$ keeps track of the stock of knowledge owned by the old member of each generation.

In continuous time, the objective function in (2.6) becomes

$$\max_{u(t)} \int_0^{\infty} e^{-\rho t} \left[\ln h(t) - \frac{c}{2} u(t)^2 \right] dt, \tag{3.4}$$

subject to the continuous-time learning function

$$\dot{h}(t) = Ah(t)^{\eta} u(t) - \delta h(t), \tag{3.5}$$

[2] As Lucas pointed out in the drafts he made for his 1988 endogenous growth theory paper (Lucas papers, Box 15), knowledge is always someone's knowledge hence it is rightly regarded as personal. Since the capacity of the human mind is limited, it cannot contain, process and apply an infinite amount of knowledge. Practically, the idea of the learning function in (3.2) is that a certain fraction of current knowledge gets out of use. Even if it remains retrievable from, for instance, documentation or other forms of technical descriptions, nobody owns it as it proved to be impractical for the current generation. The classic example of the idea is the Saturn vehicle of the Apollo Program of NASA the manufacturing of which was based on technologies and supply chains that had disappeared by today (Bilstein, 1980). The manufacturing procedures are still available in the documentation, but nobody knows today *by heart* how to build a Saturn.

where $h(t)$ and $u(t)$ denote the time paths of human capital and time investment, with $0 \leq u(t) \leq 1$.

Even if higher learning abilities run in a family that may put it on a more aggressively increasing capital profile, the high level of subjective disutility might prevent the dynasty from fulfilling its learning potential. Note that there is a trade-off between α and ζ, so a family can offset the effects of a lower α with a higher ζ. If α is assumed to be common to all families, then differences in η solely reflect differences in productivity, measured by ζ.

Therefore, in the subsequent analysis we do not need the distinction between α, ζ, and η; all attention is paid to differences in η only. Parameter η is construed to include all genetic and institutional factors (such as a supportive family environment, quiet study spaces, etc.) affecting how productively an individual uses previously acquired knowledge in human-capital accumulation. The parameter thus incorporates room for compensation between hereditary and institutional factors (Heckman, 2009).

When we subsequently form a class of students to make learning a social process, the positive effect of the class environment is modeled by an increase in η in the fashion of Lucas (1988). Parameter η itself is unobservable to the social environment of a family, while in a social setting it plays a crucial role in the selection of desired classmates. As genetics remain imperceptible to the common eye, rational families are construed to infer η from socioeconomic status. In reality, inferring η from such signals is noisy and must be considered in any model of peer selection and search leading to segregation. The present model, however, explains the drive to segregate, not segregation itself, so noise is assumed away.

Together, parameters A and η describe learning abilities and can be identified as indicators of how productively and how fast the individual accumulates human capital. The model thus draws a sharp distinction between the level of knowledge (how smart a student is) and learning ability (how fast she can learn). On this ground, the maximum attainable level of human capital

$$\bar{h} = \left(\frac{A}{\delta}\right)^{\frac{1}{1-\eta}}, \tag{3.6}$$

emerges at the intersection of the curve of maximum production of new knowledge (attained at $u = 1$) and capital loss due to depreciation. Due to diminishing marginal product of human capital, such a $\bar{h}$ exists and is unique. Obviously, $\bar{h}$ is determined by the three parameters of the learning function.

A limitation of the model must be highlighted at this early phase. Given (3.5), the rate of increase of h depends on η. At any given level of h and for a given time investment u, the sensitivity of $\dot{h}$ to η is

$$\frac{\partial \dot{h}}{\partial \eta}.$$

By requiring $\partial \dot{h}/\partial \eta > 0$ we expect a student with higher learning ability to reach a faster accumulation rate *ceteris paribus*. However, by direct calculation we obtain

$$\frac{\partial \dot{h}}{\partial \eta} = A\, h^{\eta}\, u\, \ln(h), \tag{3.7}$$

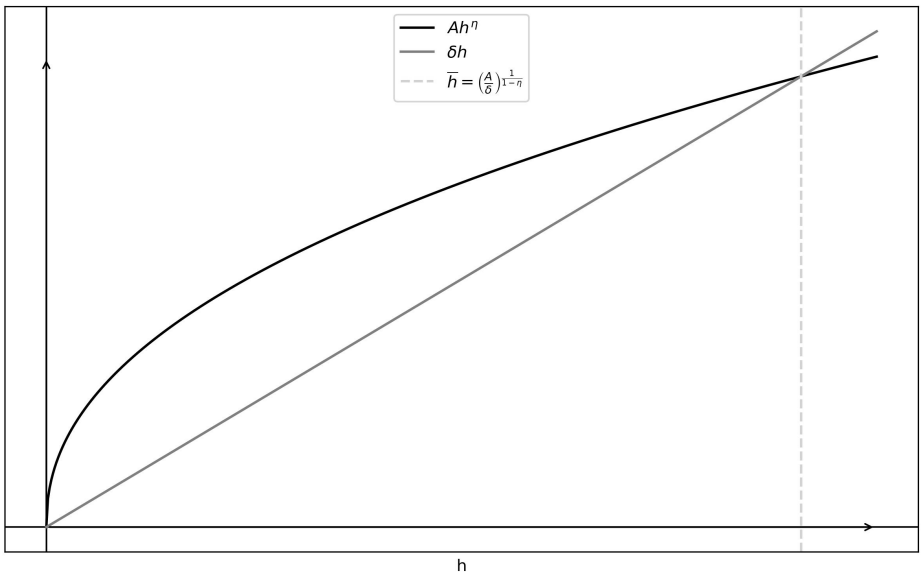


Figure 1: **Determination of the maximum capital stock. The curve Ah^η comes from (3.5) with the maximum time investment where $u = 1$ applies.**

which is negative if $0 < h < 1$ and positive for any $h > 1$. In the former case, maintaining a given rate of human-capital accumulation at the same knowledge level would require a student with higher η to invest more time than a classmate with lower η. Consequently, the model does not adequately describe human-capital accumulation at very low levels of knowledge.

This limitation is not serious for our purposes, because the model is intended to describe formal schooling, which presupposes a minimum level of prior knowledge. Empirically one may scale initial knowledge levels so that $h_0 > 1$. The process of pre-school learning could be modeled in a different framework.

The current-value Hamiltonian of the problem is

$$H(h, \theta, u) = \ln h(t) - \frac{c}{2}\, u(t)^2 + \theta(t)\big[A\, h(t)^\eta\, u(t) - \delta\, h(t)\big], \tag{3.8}$$

where $\theta(t)$ denotes the costate variable associated with $h(t)$. The necessary conditions are standard and yield the three-equation system

$$\frac{\partial H}{\partial u} = 0 \quad \Rightarrow \quad u(t) \;=\; \frac{A}{c}\,\theta(t)\, h(t)^\eta, \tag{3.9}$$

$$\dot\theta(t) \;=\; \rho\,\theta(t) - \frac{\partial H}{\partial h} \quad \Rightarrow \quad \dot\theta(t) = \theta(t)\big(\rho + \delta - A\eta\, h(t)^{\eta-1} u(t)\big) - \frac{1}{h(t)}, \tag{3.10}$$

$$\dot h(t) \;=\; A\, h(t)^\eta\, u(t) - \delta\, h(t). \tag{3.11}$$

As $h(t)$ cannot leave the state space $[0, \bar h]$, there exists a steady state (h^*, θ^*, u^*). Solving

$\dot{h} = 0$ and $\dot{\theta} = 0$ yields

$$h^* = \left[\frac{A^2}{\delta c} \cdot \frac{1}{\rho + \delta(1-\eta)} \right]^{\frac{1}{2-2\eta}}, \tag{3.12}$$

and

$$\theta^* = \frac{\delta c}{A^2} (h^*)^{1-2\eta}, \tag{3.13}$$

with u^* given by (3.9). (See Appendix A.)

4 Stability of the optimal level of knowledge

Stability of the optimal knowledge level requires h^* to be maintainable, so the necessary condition $h^* \leq \bar{h}$ must hold. As it turns out, both $h^* \leq \bar{h}$ and $u^* \leq 1$ follow if

$$\frac{\delta}{\rho + \delta(1-\eta)} \leq c, \tag{4.1}$$

holds. Condition (4.1) has a straightforward interpretation: the agent must not regard time investment as so cheap and undemanding that she would want to choose $u > 1$, which is impossible.

Just as in Ben-Porath's (1967) human-capital accumulation model, such a case can be avoided by activating the upper bound $u \leq 1$ whenever the unconstrained optimum would imply $u > 1$. As we shall see in the following section on the saddle-path analysis, $\dot{u} < 0$ can typically be expected along the entire path toward h^*, and even if $u > 1$ were to occur, it would arise only in the early phase of learning when h is low and the shadow value of human capital is high. Eventually, u falls back into the admissible range $u \leq 1$. Therefore, the constraint $u \not> 1$ may be active only temporarily.

The $\dot{h} = 0$ and $\dot{\theta} = 0$ nullclines (see Appendix A and Appendix B, respectively) take different shapes depending on η. For stability reasons the case $0.5 < \eta < 1$ proves to be irrelevant. However, when $0 < \eta < 0.5$ the system is saddle-path stable, so for any $1 < h_0 < h^*$ there exists a unique $\theta(0)$ from which the stock of knowledge converges to the steady state h^* (see Appendix C).

A simple calibration method is available to handle the limitation arising when some estimated η would fall into the $0.5 < \eta < 1$ range. Suppose h_0 (the starting value) and h_1 (the terminal value) are estimated from school test data for a class or cohort, and suppose an aggregate time investment $u_0 \in [0, 1]$ summarizing the learning period is known from survey results. Then there are two free parameters, A and η, to calibrate. Using (3.3) one can solve for individual η values given a common $A > 0$. Since η depends inversely on A, a simple iterative procedure is to start with a sufficiently low $A > 0$ and increase A stepwise until the largest implied η falls below 0.5 while preserving $0 < \eta$ for all individuals.

In more heterogeneous cohorts this procedure may fail: forcing the largest η below 0.5 might require some individual η to become nonpositive, which indicates that the assumption of a single common A across the cohort is not tenable. That heterogeneity in A is precisely what we abstract from for simplicity in the present analysis.

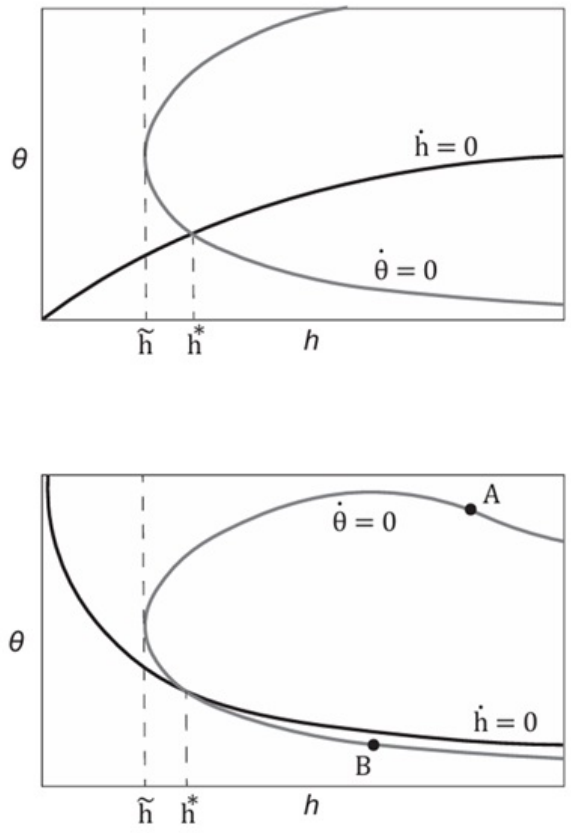


Figure 2: **Typical shapes of the nullclines with $0 < \eta < 0.5$ on the upper pane, and $0.5 < \eta < 1$ on the lower pane. The lower pane also includes a schematic representation of the ambiguity of the $0.5 < \eta < 1$ case. In point A, moving to the left we eventually get to the right of the $\dot{\theta} = 0$ nullcline. Likewise, in point B, moving upwards we eventually get under the same nullcline.**

5 Saddle path analysis

As learning is a timely process, the representative agent's utility depends both on the level of the steady-state capital stock h^* and its maintenance costs u^*, and on the optimal path toward the equilibrium. Therefore, attention must be paid to the characteristics of this path. In this section we characterize the optimal path of the capital stock.

Because the model features a convex cost function, an important question concerns the concavity of the optimal path. A large literature, initiated by Eisner and Strotz (1962) and followed by early work of Lucas (1965a,b,c), shows that convex costs encourage postponing investment: although the agent could choose a sharp increase in the state variable at any instant, it is typically cheaper to expand more slowly, which yields concavity of the optimal capital path. In the present model the sign of $\ddot{h}$ is not unambiguously negative, so some convexity in the early phases of human-capital accumulation cannot be excluded. Such a convex section signals that the representative agent prefers rapid initial learning.

The model establishes a close relationship between η and the initial shadow value $\theta(0)$.

Given h_0, a higher η raises h^* and tends to increase $\theta(0)$ (see Appendix D).[3] To see this, note that the isoquant curves of the learning function in (3.5) shift differently at different values of h. From (3.5) the dynamic isoquants for a given $\dot{h} > 0$ take the form

$$\frac{\dot{h} - \delta h}{A h^{\eta}} \equiv f(h) = u,$$

and for a starting value h_0 sufficiently close to 1 an increase in η does not make it much easier to reach and maintain a given $\dot{h}$. While a higher η raises h^*, starting from a low $h_0 > 1$ the agent cannot rely on improved learning ability to achieve higher $\dot{h}$ in the early stage. Because a change in η alters the curvature of the isoquants in this region (see Fig. 3), achieving a higher h^* with higher accumulation rates requires more time investment. Hence an increase in η does not alleviate the scarcity of h_0, so higher η tends to increase $\theta(0)$; formally, $\partial\theta(0)/\partial\eta > 0$ at low h_0.

By contrast, an increase in A shifts each isoquant downward, making it easier to maintain a given $\dot{h}$. Thus, even though h^* increases with A and h_0 becomes relatively scarcer, a larger A eases scarcity at low h_0, so $\partial\theta(0)/\partial A < 0$. In later phases of accumulation an increase in η becomes more valuable than an increase in A, because higher η allows maintaining given $\dot{h}$ at smaller time investments. Simulation results support this pattern.

These insights imply that by decreasing $h_0 > 1$ and increasing η we may induce the representative agent to learn more aggressively, thereby producing a starting value for the optimal human-capital accumulation process that exhibits an initial convex section. Figure 4 shows that increasing η indeed generates initial convexity, which disappears as η takes lower values.

It is straightforward to show from (3.9) that

$$\dot{u}(t) = \frac{A}{c}\Big[\dot{\theta}(t)\, h(t)^{\eta} + \eta\, \theta(t)\, h(t)^{\eta-1}\, \dot{h}(t)\Big], \tag{5.1}$$

which, after substituting the expressions for $\dot{\theta}(t)$ and $\dot{h}(t)$, yields

$$\dot{u}(t) = \frac{A}{c}\,\theta(t)\, h(t)^{\eta}\big(\rho + \delta(1-\eta)\big) - \frac{A}{c}\, h(t)^{\eta-1}. \tag{5.2}$$

Hence $\dot{u}(t) < 0$ (so $u(t)$ is decreasing) as long as

$$\theta(t) \;<\; \frac{1}{\rho + \delta(1-\eta)} \cdot \frac{1}{h(t)}. \tag{5.3}$$

Time investment therefore depends on the relationship between θ and h, and $u(t)$ may increase if the inequality in (5.3) is reversed. Because the first term on the right-hand side of (5.2) is typically large, in most parameter configurations one finds $\dot{u} < 0$.

To search for parameter configurations that might produce $\dot{u} > 0$ at least temporarily, we ran a grid search over the hyperrectangle

$$A \in [0.2, 10], \quad c \in [1, 120], \quad \delta \in [0.01, 0.4], \quad \eta \in [0.1, 0.45], \quad \rho \in [0.01, 0.1],$$

[3] Consequently, an agent with superior learning abilities attains a higher steady-state knowledge level, h^*. Because the absolute depreciation of knowledge, δh^*, is proportionally larger at this elevated state, the agent must continuously generate a greater volume of new knowledge to offset the loss. Thus, the model implies that higher-ability individuals consistently exhibit higher absolute rates of knowledge production.

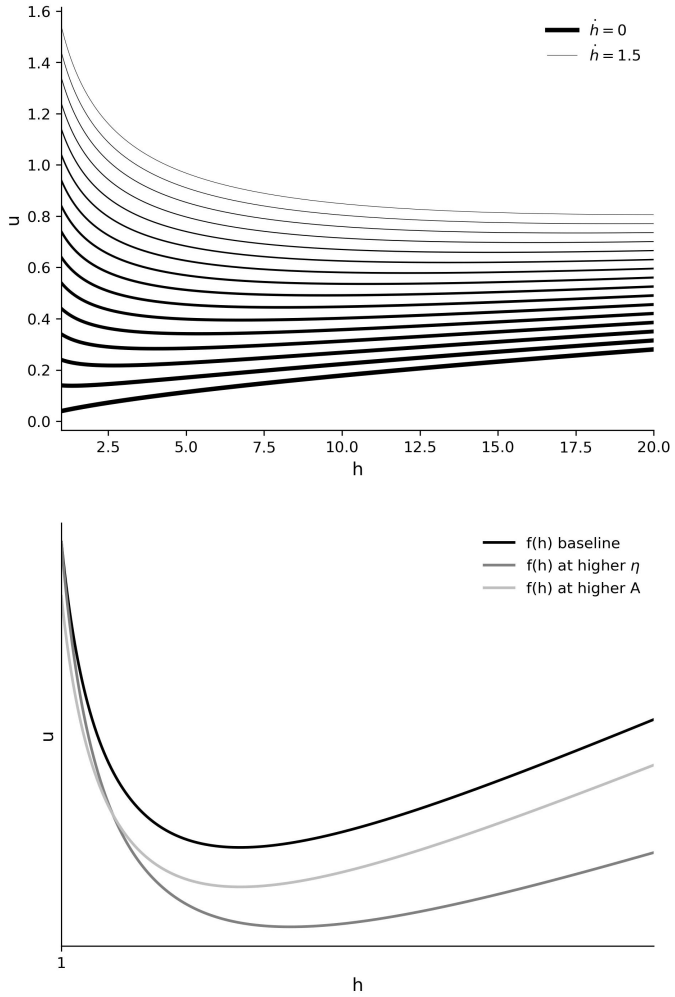


Figure 3: **The isoquant map of the learning function (upper pane, where $A = 1$ and $\delta = 0.04$); and the typical effects of a change in η or A on the shape of the learning function (lower pane, parameters being the same). Most importantly, as the lower pane shows, at low levels of $h_0 > 1$ an increase in A reduces the time needed for maintaining a given value of $\dot{h}$ more than an increase in η.**

which corresponds to 25,000 simulation runs. None of these experiments produced cases with $\dot{u}(t) > 0$. Analytical and numerical solutions show that time investment yields the highest marginal return at $t = 0$, with the optimal path of $u(t)$ being strictly decreasing thereafter across the entire feasible parameter space.

Beyond the strictly decreasing nature of $u(t)$, the model reveals a fundamental structural property regarding the cross-sectional distribution of optimal time investment. Conventional pedagogical narratives often frame effort as a compensatory mechanism, assuming that less capable students invest more time to offset their lower cognitive endowments. However, our framework dictates the exact opposite. As demonstrated by the time trajectories in Figure 5 and the exact numerical evaluations in Table 1, the optimal time investment $u(t)$ is strictly increasing in the learning ability parameter η at every point in time.

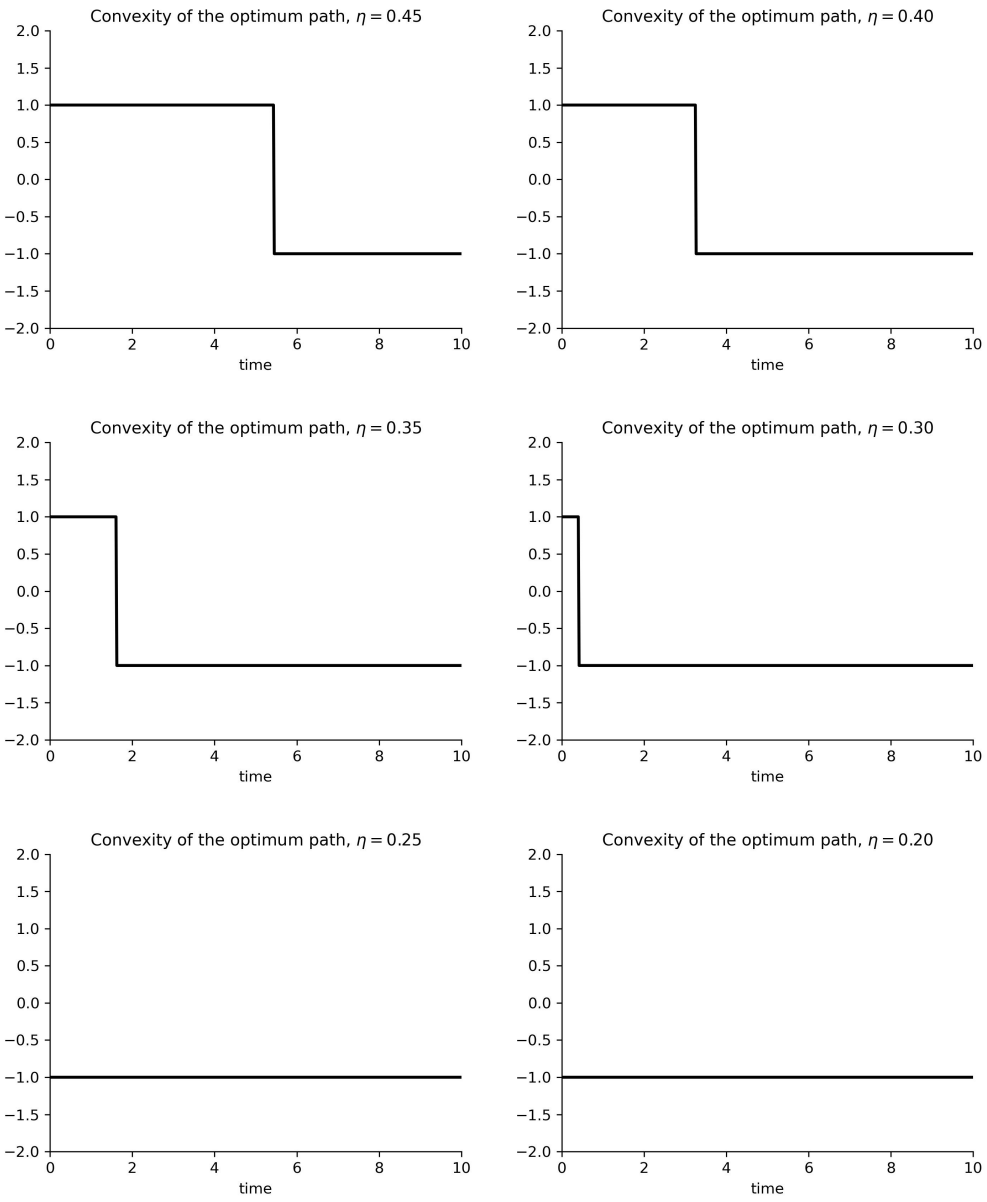


Figure 4: **Convex sections of the optimum path of $h(t)$ at different values of η. The parameter vector is $[A, c, \delta, \rho] = [1, 5, 0.04, 0.05]$. Appendix D describes the formal criterion of convexity whose sign we use in simulation; a positive sign, indicated by the signum of the criterion, denotes convexity.**

This endogenous nature of effort is most starkly illuminated by the policy functions in Figure 6. Even when controlling for the level of accumulated human capital, the optimal policy of a higher-η agent consistently commands greater time investment. A highly capable agent exerts massive effort not due to an exogenous moral virtue like diligence, but strictly because their internal human capital accumulation machinery yields superior marginal returns. The agent with lower cognitive endowments rationally chooses to invest less time and exit the intense accumulation phase earlier, definitively rejecting the compensatory hypoth-

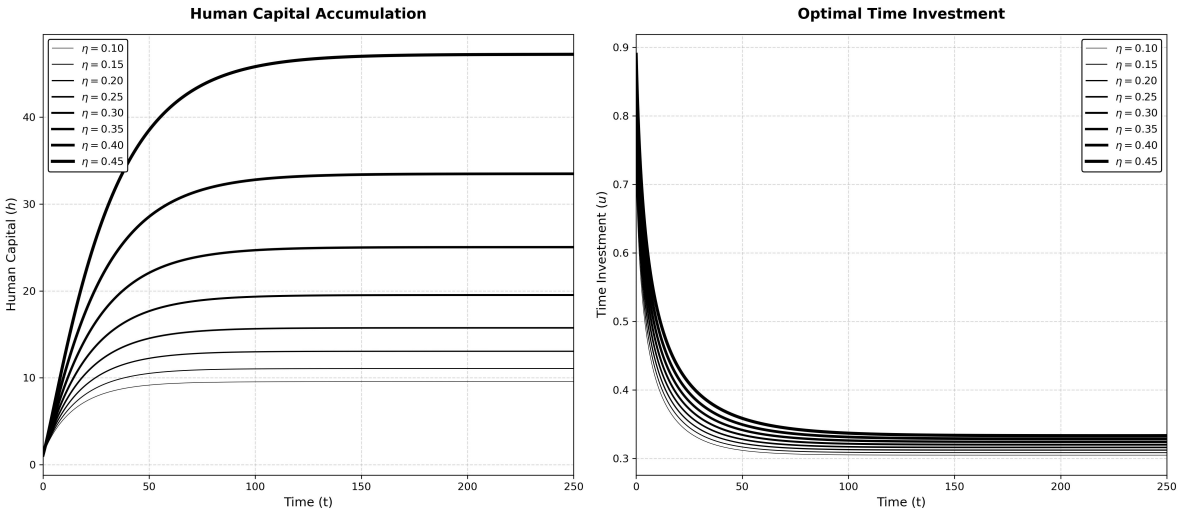


Figure 5: **Human capital accumulation (left) and the optimal time investment trajectories (right) over time for varying levels of η. Thicker lines correspond to higher values of η (ranging from 0.10 to 0.45). Higher learning ability systematically dictates a massively higher time investment throughout the entire transition path. The parameter vector is $[A, c, \delta, \rho] = [1, 5, 0.04, 0.05]$.**

Table 1: **Optimal time investment $u(t)$ evaluated at discrete time points across varying learning ability (η) parameters. The data confirms that higher η unambiguously shifts the entire $u(t)$ trajectory upwards. The parameter vector is $[A, c, \delta, \rho] = [1, 5, 0.04, 0.05]$.**

t	$\eta = 0.10$	$\eta = 0.15$	$\eta = 0.20$	$\eta = 0.25$	$\eta = 0.30$	$\eta = 0.35$	$\eta = 0.40$	$\eta = 0.45$
0	0.716452	0.735513	0.756030	0.778213	0.802316	0.828654	0.857625	0.889736
25	0.338008	0.345459	0.353594	0.362528	0.372402	0.383394	0.395734	0.409723
50	0.311951	0.316896	0.322252	0.328093	0.334513	0.341634	0.349613	0.358659
75	0.306605	0.310662	0.314982	0.319612	0.324615	0.330074	0.336101	0.342847
100	0.305376	0.309128	0.313066	0.317219	0.321629	0.326350	0.331456	0.337053
125	0.305087	0.308740	0.312545	0.316521	0.320693	0.325096	0.329778	0.334809
150	0.305018	0.308641	0.312402	0.316314	0.320396	0.324667	0.329161	0.333922
175	0.305002	0.308615	0.312362	0.316253	0.320301	0.324520	0.328933	0.333569
200	0.304998	0.308609	0.312352	0.316235	0.320271	0.324470	0.328848	0.333429
225	0.304997	0.308607	0.312349	0.316230	0.320262	0.324454	0.328822	0.333384
250	0.304998	0.308608	0.312350	0.316233	0.320268	0.324468	0.328855	0.333461

esis.

Note that an initially convex capital path may include sections where $u(t) > 1$; in such cases the upper bound $u(t) \leq 1$ must be enforced. Uniqueness and saddle-path stability continue to hold in these constrained cases (see Appendix E).

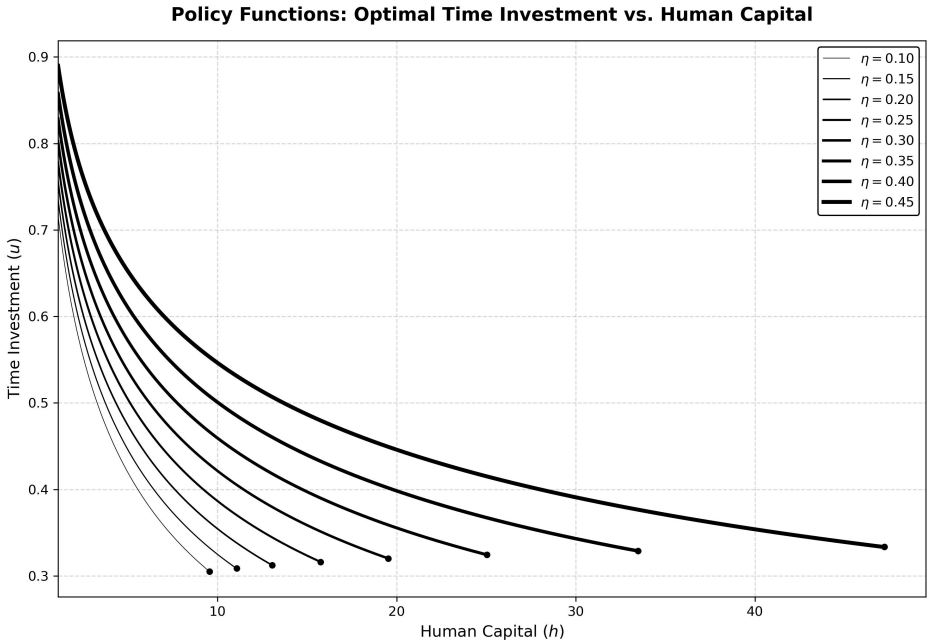


Figure 6: **Policy functions mapping optimal time investment u against the accumulated human capital h. Black dots indicate the steady-state equilibrium (h^*, u^*) for each corresponding η. Even at identical levels of human capital, agents with higher learning ability optimally choose higher time investment. The parameter vector is $[A, c, \delta, \rho] = [1, 5, 0.04, 0.05]$.**

6 Learning as a social activity

After characterizing the problem of the infinitely living representative agent taken as an isolated family, in Sections 6–7 we turn human capital accumulation into a social problem. Practically, we do this by introducing an external effect into the learning function to describe how learning abilities interplay in communities. With an external effect, however, we must distinguish equilibrium and optimum solutions. Following Lucas (1988) and Romer (1986), the equilibrium paths of $h(t)$ and $u(t)$ directly result from the solutions of the isolated problems. In equilibrium, families forming a community optimize individually. Even if the individual representing a dynasty knows that her own learning process is affected by how others accumulate human capital, having no control over these processes she treats these paths as exogenously given. Note that there is no market interaction in this setting: human capital is not traded, it only externally affects the learning processes in a community. The social optimum, by contrast, is established by the social planner, here interpreted as a schoolteacher who has full control over the time investment of each student in the class and simultaneously plans optimal paths for all members of the community.

The external effect modifies the individual's learning function in a way that closely resembles the way Lucas (1988, p. 18) introduced knowledge externalities into commodity production. Instead of describing average knowledge with an arithmetic mean, we use the geometric mean to preserve the multiplicative relationship in the learning function. To keep things simple, we work with two individuals indexed by 1 and 2, so the average knowledge

level is

$$h_a(t) = \sqrt{h_1(t)\, h_2(t)}, \tag{6.1}$$

and the learning equations (cf. (3.5)) become

$$\dot{h}_1(t) = A\, h_a(t)^{\gamma}\, h_1(t)^{\eta_1} u_1(t) - \delta\, h_1(t) \tag{6.2a}$$

$$\dot{h}_2(t) = A\, h_a(t)^{\gamma}\, h_2(t)^{\eta_2} u_2(t) - \delta\, h_2(t) \tag{6.2b}$$

We allow η_1 and η_2 to differ, and $\gamma > 0$ is the parameter that captures the external effect of human capital accumulation. Obviously, γ can be interpreted as reflecting the overall quality of the learning environment: a better school corresponds to a higher γ. Further specifications will be introduced later. When $\gamma = 0$ we recover the isolated-individual problem. Without loss of generality assume $0 < \eta_2 < \eta_1 < 0.5$, so dynasty 1 has higher learning ability than dynasty 2.

Noting that $h_a(t)$ depends on each individual's knowledge level, we can rewrite (6.2a) and (6.2b) as

$$\begin{aligned} \dot{h}_1(t) &= A\, h_1(t)^{\gamma/2}\, h_2(t)^{\gamma/2}\, h_1(t)^{\eta_1}\, u_1(t) - \delta\, h_1(t) \\ &= A\, h_2(t)^{\gamma/2}\, h_1(t)^{\eta_1+\gamma/2}\, u_1(t) - \delta\, h_1(t), \end{aligned} \tag{6.3a}$$

$$\begin{aligned} \dot{h}_2(t) &= A\, h_1(t)^{\gamma/2}\, h_2(t)^{\gamma/2}\, h_2(t)^{\eta_2}\, u_2(t) - \delta\, h_2(t) \\ &= A\, h_1(t)^{\gamma/2}\, h_2(t)^{\eta_2+\gamma/2}\, u_2(t) - \delta\, h_2(t). \end{aligned} \tag{6.3b}$$

From the viewpoint of each individual the fellow student's capital enters as an exogenous multiplicative factor, so the problem can be reduced to the isolated case with effective parameters $A\, h_j(t)^{\gamma/2}$ and $\eta_i + \gamma/2$ (for $i, j \in \{1, 2\}$, $i \neq j$). Thus the external effect effectively raises each individual's learning parameter to $0 < \eta_i + \gamma/2 < 0.5$ under the maintained assumptions. Equilibrium knowledge levels are finite because there are upper bounds on the set of feasible capital stocks (see Appendix F).

Under the previous assumptions, the current-value Hamiltonians of the individuals in the equilibrium setting are

$$\widehat{H}_1(h_1, \theta_1, u_1) = \ln h_1 - \frac{c}{2} u_1^2 + \theta_1 \big(A\, h_2^{\gamma/2}\, h_1^{\eta_1+\gamma/2}\, u_1 - \delta\, h_1 \big), \tag{6.4a}$$

$$\widehat{H}_2(h_2, \theta_2, u_2) = \ln h_2 - \frac{c}{2} u_2^2 + \theta_2 \big(A\, h_1^{\gamma/2}\, h_2^{\eta_2+\gamma/2}\, u_2 - \delta\, h_2 \big). \tag{6.4b}$$

Each individual's problem is thus a version of (3.8) with effective parameters $A\, h_j(t)^{\gamma/2}$ and $\eta_i + \gamma/2$ in the learning function. Treating the fellow student's capital as exogenous, the

equilibrium stocks h_1^e and h_2^e satisfy the fixed-point system

$$h_1^e = \left[\frac{\dfrac{A^2}{\delta c}\,(h_2^e)^\gamma}{\rho + \delta\big(1 - \eta_1 - \gamma/2\big)} \right]^{\frac{1}{2-2(\eta_1+\gamma/2)}}, \tag{6.5a}$$

$$h_2^e = \left[\frac{\dfrac{A^2}{\delta c}\,(h_1^e)^\gamma}{\rho + \delta\big(1 - \eta_2 - \gamma/2\big)} \right]^{\frac{1}{2-2(\eta_2+\gamma/2)}}. \tag{6.5b}$$

Consequently, the equilibrium costate values are

$$\theta_1^e = \frac{\delta c}{A^2(h_2^e)^\gamma} \left[\frac{\dfrac{A^2(h_2^e)^\gamma}{\delta c}}{\rho + \delta\big(1 - \eta_1 - \gamma/2\big)} \right]^{\frac{1-2(\eta_1+\gamma/2)}{2-2(\eta_1+\gamma/2)}}, \tag{6.6}$$

$$\theta_2^e = \frac{\delta c}{A^2(h_1^e)^\gamma} \left[\frac{\dfrac{A^2(h_1^e)^\gamma}{\delta c}}{\rho + \delta\big(1 - \eta_2 - \gamma/2\big)} \right]^{\frac{1-2(\eta_2+\gamma/2)}{2-2(\eta_2+\gamma/2)}}. \tag{6.7}$$

Solving the fixed-point problem yields the closed-form equilibrium knowledge levels

$$h_1^e = \left[\frac{A^2/(\delta c)}{\rho + \delta(1 - \eta_1 - \gamma/2)} \right]^{\frac{2-2\eta_2-\gamma}{D}} \left[\frac{A^2/(\delta c)}{\rho + \delta(1 - \eta_2 - \gamma/2)} \right]^{\frac{\gamma}{D}}, \tag{6.8a}$$

$$h_2^e = \left[\frac{A^2/(\delta c)}{\rho + \delta(1 - \eta_2 - \gamma/2)} \right]^{\frac{2-2\eta_1-\gamma}{D}} \left[\frac{A^2/(\delta c)}{\rho + \delta(1 - \eta_1 - \gamma/2)} \right]^{\frac{\gamma}{D}}, \tag{6.8b}$$

where

$$D \;=\; (2\eta_1 + \gamma - 2)(2\eta_2 + \gamma - 2) - \gamma^2. \tag{6.9}$$

Thus h_1^e depends on η_2: the student with inferior learning ability affects her classmate's equilibrium stock. When $\eta_1 = \eta_2 \equiv \eta$ we recover $h_1^e = h_2^e$. It can be shown that, under a wide range of parameter configurations, both equilibrium stocks h_1^e and h_2^e increase with η_1 and η_2 (see Appendix G).

One can view the equilibrium problem in the class as an infinite chain of isolated problems. From the viewpoint of Student 1, the classmate's capital enters the learning function as a multiplicative factor $A\,h_2(t)^{\gamma/2}$, so Student 1's equilibrium problem is analogous to an isolated problem with an exogenously increasing A. Recall that for any appropriate parameter configurations the isolated case is saddle-path stable with $\dot{h} > 0$; hence for any exogenous $h_2(0)$ the knowledge level $h_1(0)$ starts growing (so $\dot{h}_1(0) > 0$), and symmetrically for Student 2.

At the start of the learning process ($t = 0$), with $h_1(0)$ and $h_2(0)$ given, Student 1 converges along a stable manifold toward the temporary endpoint

$$\vec{h}_1(0) = \left[\frac{\left(A\, h_2(0)^{\gamma/2}\right)^2/(\delta c)}{\rho + \delta\big(1 - \eta_1 - \gamma/2\big)} \right]^{\frac{1}{2-2(\eta_1+\gamma/2)}}, \tag{6.10}$$

which is the analogue of (6.5a) with $h_2(0)$ treated as given. The temporary endpoint for Student 2 is defined analogously with $h_1(0)^{\gamma/2}$ entering the expression:

$$\vec{h}_2(0) = \left[\frac{\left(A\, h_1(0)^{\gamma/2}\right)^2/(\delta c)}{\rho + \delta\big(1 - \eta_2 - \gamma/2\big)} \right]^{\frac{1}{2-2(\eta_2+\gamma/2)}}. \tag{6.11}$$

Because $h_2(t)$ also increases under saddle-path stability, these temporary endpoints evolve over time; denote them by $\vec{h}_i(t)$ and $\vec{\theta}_i(t)$ for $i = 1, 2$ at any time t. For each t the pair $(\vec{h}_i(t), \vec{\theta}_i(t))$ is a temporary steady state with a unique associated stable manifold. Thus students converge to moving targets, shifting from one temporary saddle path to the next and moving toward the lower-right corner of the phase diagrams (see Fig. 10 in Appendix C). Moreover,

$$\lim_{t\to\infty} \vec{h}_i(t) = h_i^e,$$

with h_i^e given by the equilibrium expressions in (6.5a)–(6.5b) (or by the closed forms in (6.8a)–(6.8b)). The phase diagram of each individual's equilibrium problem is therefore a time-indexed family of phase diagrams: the state converges toward h_i^e while the temporary saddle path continuously shifts.

It is also straightforward to verify that h_i^e coincides with the isolated-case steady state h^* computed with an effective productivity $A(h_j^e)^{\gamma/2}$ and an effective learning parameter $\eta + \gamma/2$. In this section we only establish that at every point in time each agent has a stable manifold and converges by moving from one saddle path to the next; how this moving-target convergence affects the social optimum is addressed in Section 7.

As we reduce the equilibrium dynamics to the isolated-individual case, it is useful to examine how the endpoints of convergence shift. Regarding comparative statics, note that the condition

$$\frac{A^2/(\delta c)}{\rho + \delta(1-\eta)} > 1 \tag{6.12}$$

is the relevant requirement for $h^* > 1$. Hence higher learning ability η leads to a higher optimal knowledge level. For typical parameter values one also finds $\partial\theta^*/\partial\eta < 0$, reflecting that individuals with higher learning ability place a lower shadow value on an additional unit of knowledge. Rewriting θ^* as

$$\theta^* = \big[\rho + \delta(1-\eta)\big]^{\frac{2\eta-1}{2-2\eta}} \left(\frac{\delta c}{A^2}\right)^{\frac{1}{2-2\eta}}, \tag{6.13}$$

a sufficient (but not necessary) condition for θ^* to decrease in η is that each factor on the right decreases in η. The sign of the differential of the first factor is negative if

$$\ln\big[\rho+\delta(1-\eta)\big]+\frac{\delta(2\eta-1)(2\eta-2)}{2\big[\rho+\delta(1-\eta)\big]}<0 \tag{6.14}$$

holds for $0<\eta<0.5$. The second factor on the left is strictly convex approaching zero when $\eta\to 0.5$, and approaching $\delta/(\rho+\delta)>0$ when $\eta\to 0$, so its supremum is $\delta/(\rho+\delta)$ over $\eta=0$. The first factor is strictly decreasing in η, and its supremum is $\ln(\rho+\delta)$ over $\eta=0$. As each term has its supremum over $\eta=0$, the supremum of the whole expression is here. A convenient sufficient condition for (6.14) is

$$f(\delta,\rho)\equiv\ln[\rho+\delta]+\frac{\delta}{\rho+\delta}<0, \tag{6.15}$$

where $f(\delta,\rho)$ is strictly increasing in both arguments and tends to $-\infty$ as $\delta\to 0$ and $\rho\to 0$. Figure 7 (right pane) illustrates the curve $f(\delta,\rho)=0$, which divides the (δ,ρ)-space; positive values of f lie to the right of the curve.

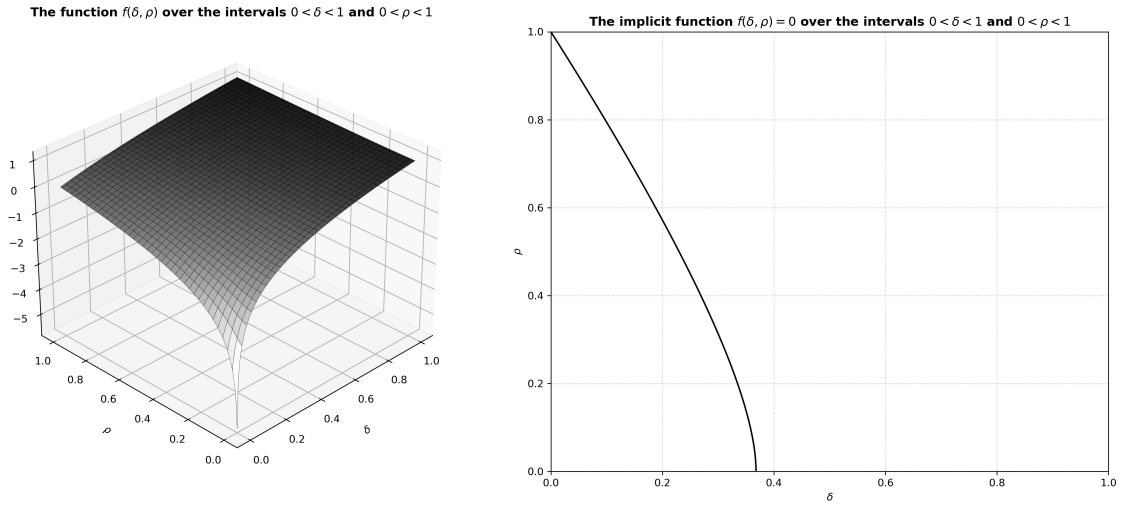


Figure 7: **The function $f(\delta,\rho)$ over the intervals $0<\delta<1$ and $0<\rho<1$ (left pane), and the implicit function $f(\delta,\rho)=0$ over the same intervals (right pane).**

As the figure suggests, the inequality in (6.15) holds for a wide range of normal values for δ at normally low levels of ρ. Due to sufficiency, (6.14) holds for a wider range of parameters than for which (6.15) holds.

In the second factor for θ^*, direct differentiation shows the exponent $0.5<(2-2\eta)^{-1}<1$ to be increasing in η, so the whole term is a decreasing function of η as long as $A^2>\delta c$. However, for high values of c, $\partial\theta^*/\partial\eta>0$ *might* occur since the monotonicity of θ^* in η depends on the monotonicity of the two terms taken together. Even if the first term drops in response to an increase in η, the second term might offset it by a sharper increase.

By the same direct calculation of the differentials of h^* (Appendix A) for the $0<\eta<0.5$ case, we also have $\partial h^*/\partial c<0$, so higher subjective costs prevent the representative agent from fulfilling her potential in learning, as we expected at the outset. No matter how quickly a student could learn, suffering from the daily chores of mugging at home discourages her

Table 2: **Signs of the partial differentials of h^* and θ^* with respect to the parameters of the problem.**

Parameter	$\partial h^*/\partial(\cdot)$	$\partial\theta^*/\partial(\cdot)$
η	> 0	$\pm$
A	> 0	< 0
c	< 0	> 0
δ	< 0	> 0

from learning. The table below summarizes the first-order partial differentials of the steady-state values with respect to the parameters.

Therefore, the equilibrium allocation to which the system converges as a sequence of temporary equilibria moves to the bottom right as $\partial h^*/\partial A > 0$ and $\partial\theta^*/\partial A < 0$, while the sign of $\partial\theta^*/\partial\eta$ is uncertain, so the effect on the endpoint of a rise in η due to the additive increase from γ in the social setting is not clear in cases where c is 'extremely' high. For 'normally' high values of c we can expect $\partial\theta^*/\partial\eta < 0$ to hold. The stability of the equilibrium dynamics directly follows from the stability of the dynamics of the isolated individual: At any point in time and at any exogenously given human capital of the classmate, the individual's capital stock converges toward a stable capital stock (Appendix H).

To fully appreciate the dynamics of this decentralized equilibrium, we must examine the transition paths. As Table 4 and Figure 8 illustrate, the response of a high-ability agent to their peer's capacity (η_2) is profoundly non-linear over time, reflecting a sophisticated intertemporal substitution. At $t = 0$, facing identical initial capital stocks ($h_1(0) = h_2(0) = 1.1$), the optimal time investment $u_1(0)$ is strictly decreasing in the peer's ability.

Because initial capital levels are fixed, this early response is driven purely by the shadow price $\theta_1(0)$. As Table 3 explicitly demonstrates, the shadow price $\theta_1(t)$ is a strictly decreasing function of the peer's ability η_2 at every point in time. Crucially, this mechanism is in perfect harmony with the logic of the isolated case. In isolation, a higher personal learning ability increases the scarcity of the fixed initial stock relative to the attainable steady state, thereby raising the initial shadow price and prompting intense early effort. In the social equilibrium, the agent effectively treats the classmate as a structural determinant of their own capital's scarcity. A highly capable peer promises abundant future knowledge spillovers, which structurally lowers the scarcity of human capital within the learning environment and immediately depresses the shadow value of the agent's own capital. This lower shadow price mathematically dictates the reduction in initial effort.

However, as the capital stocks evolve ($t \geq 50$), this dynamic entirely reverses (see Figure 8). The physical accumulation of capital begins to dominate the shadow price. The multiplicative peer effect ($h_2^{\gamma/2}$) acts as an increasingly powerful amplifier for the high-ability peer, drastically raising the marginal product of the agent's own time investment. Consequently, the optimal time investment $u_1(t)$ becomes strictly increasing in the peer's ability. The compensatory hypothesis fails once again: the high-ability student eventually invests less time when paired with a low-ability peer not out of complacency, but because the inferior peer acts as a drag on the learning machinery's efficiency, rationally discouraging further

Table 3: **Shadow price $\theta_1(t)$ of the high-ability agent ($\eta_1 = 0.45$) paired with varying peers. The shadow price remains strictly decreasing in the peer's learning ability η_2 at all points in time, reflecting the continuously reduced scarcity of human capital in a high-synergy environment. The parameter vector is $[A, c, \delta, \gamma, \rho] = [1, 5, 0.04, 0.2, 0.05]$.**

t	$\eta_2 = 0.10$	$\eta_2 = 0.15$	$\eta_2 = 0.20$	$\eta_2 = 0.25$	$\eta_2 = 0.30$	$\eta_2 = 0.35$	$\eta_2 = 0.40$
0	4.264492	4.249712	4.233364	4.215164	4.194757	4.171682	4.145335
5	0.838022	0.829807	0.820765	0.810753	0.799594	0.787059	0.772851
10	0.415509	0.408629	0.401064	0.392700	0.383393	0.372965	0.361185
20	0.201166	0.196024	0.190391	0.184193	0.177338	0.169714	0.161178
50	0.091174	0.087614	0.083745	0.079530	0.074923	0.069875	0.064330
100	0.065992	0.062840	0.059426	0.055723	0.051704	0.047339	0.042603
200	0.060489	0.057364	0.053974	0.050293	0.046296	0.041958	0.037260
300	0.060187	0.057055	0.053655	0.049962	0.045947	0.041584	0.036854
400	0.060172	0.057039	0.053638	0.049943	0.045926	0.041561	0.036827

investment.

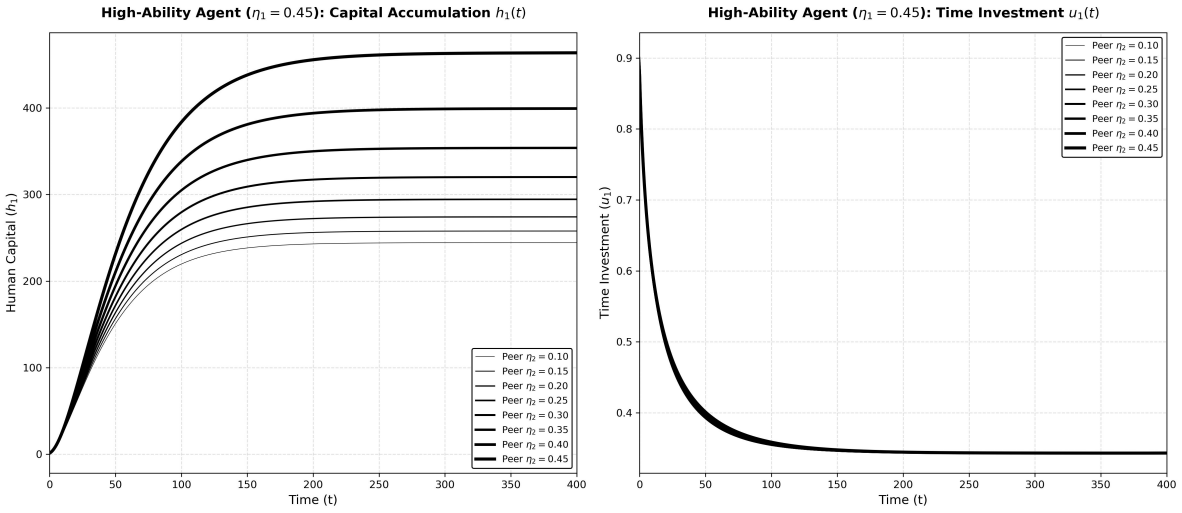


Figure 8: **Capital accumulation (left) and optimal time investment (right) for a high-ability agent ($\eta_1 = 0.45$) matched with peers of varying abilities ($\eta_2 \in [0.10, 0.40]$) in the decentralized equilibrium. Extended time horizon ($T = 400$) ensures complete convergence to the respective steady states. The parameter vector is $[A, c, \delta, \gamma, \rho] = [1, 5, 0.04, 0.2, 0.05]$.**

We can find the social optimum with the external effect by solving the current-value Hamiltonian

Table 4: **High-Ability Agent ($\eta_1 = 0.45$) optimal time investment $u_1(t)$ paired with varying peers. The data highlights the intertemporal substitution: higher peer ability suppresses initial effort via lower shadow prices but strictly amplifies effort in later stages as human capital synergies dominate. The parameter vector is $[A, c, \delta, \gamma, \rho] = [1, 5, 0.04, 0.2, 0.05]$.**

t	$\eta_2 = 0.10$	$\eta_2 = 0.15$	$\eta_2 = 0.20$	$\eta_2 = 0.25$	$\eta_2 = 0.30$	$\eta_2 = 0.35$	$\eta_2 = 0.40$
0	0.907408	0.904263	0.900784	0.896912	0.892569	0.887659	0.882053
50	0.390964	0.391826	0.392813	0.393954	0.395283	0.396850	0.398721
100	0.353512	0.353878	0.354313	0.354836	0.355469	0.356246	0.357212
150	0.345502	0.345631	0.345792	0.345993	0.346248	0.346578	0.347011
200	0.343602	0.343643	0.343696	0.343765	0.343857	0.343982	0.344156
250	0.343144	0.343156	0.343172	0.343194	0.343225	0.343268	0.343333
300	0.343033	0.343036	0.343041	0.343048	0.343057	0.343072	0.343095
350	0.343006	0.343007	0.343009	0.343011	0.343014	0.343019	0.343027
400	0.343017	0.343020	0.343024	0.343030	0.343039	0.343055	0.343084

$$\widetilde{H}(h_1, h_2, \theta_1, \theta_2, u_1, u_2) = \ln h_1 + \ln h_2 - \frac{c}{2}u_1^2 - \frac{c}{2}u_2^2 + \theta_1\big(A h_2^{\gamma/2} h_1^{\eta_1+\gamma/2} u_1 - \delta h_1\big) + \theta_2\big(A h_1^{\gamma/2} h_2^{\eta_2+\gamma/2} u_2 - \delta h_2\big). \tag{6.16}$$

Just like previously, when $\gamma = 0$ human capital accumulation is not affected by the classmate's knowledge; the two problems decouple and the social planner solves two separate isolated problems. Following the standard procedure, the necessary first-order conditions and the costate/state dynamics yield the six-equation system below.

$$u_1 = \frac{A}{c}\,\theta_1\, h_2^{\gamma/2}\, h_1^{\eta_1+\gamma/2}, \tag{6.17a}$$

$$u_2 = \frac{A}{c}\,\theta_2\, h_1^{\gamma/2}\, h_2^{\eta_2+\gamma/2}, \tag{6.17b}$$

$$\dot{\theta}_1 = (\rho+\delta)\theta_1 - \frac{1}{h_1} - A(\eta_1+\gamma/2)\,\theta_1\, h_1^{\eta_1+\gamma/2-1}\, h_2^{\gamma/2}\, u_1 - A\frac{\gamma}{2}\,\theta_2\, h_1^{\gamma/2-1}\, h_2^{\eta_2+\gamma/2}\, u_2, \tag{6.17c}$$

$$\dot{\theta}_2 = (\rho+\delta)\theta_2 - \frac{1}{h_2} - A(\eta_2+\gamma/2)\,\theta_2\, h_1^{\gamma/2}\, h_2^{\eta_2+\gamma/2-1}\, u_2 - A\frac{\gamma}{2}\,\theta_1\, h_1^{\eta_1+\gamma/2}\, h_2^{\gamma/2-1}\, u_1, \tag{6.17d}$$

$$\dot{h}_1 = A\, h_2^{\gamma/2}\, h_1^{\eta_1+\gamma/2}\, u_1 - \delta\, h_1, \tag{6.17e}$$

$$\dot{h}_2 = A\, h_1^{\gamma/2}\, h_2^{\eta_2+\gamma/2}\, u_2 - \delta\, h_2. \tag{6.17f}$$

In steady state we set $\dot{h}_1 = \dot{h}_2 = \dot{\theta}_1 = \dot{\theta}_2 = 0$. Substituting (6.17a)–(6.17b) into the state equations (6.17e)–(6.17f) and imposing $\dot{h}_1 = \dot{h}_2 = 0$ yields expressions for the steady-state

costates:

$$\theta_1 = \frac{\delta c}{A^2}\, h_1^{1-2\eta_1-\gamma}\, h_2^{-\gamma}, \tag{6.18a}$$

$$\theta_2 = \frac{\delta c}{A^2}\, h_1^{-\gamma}\, h_2^{1-2\eta_2-\gamma}. \tag{6.18b}$$

Substituting (6.18) into the costate steady-state conditions $\dot{\theta}_1 = \dot{\theta}_2 = 0$ reduces the system to two equations in h_1 and h_2. Working with these and exploiting the system's symmetries yields an Euler-type relation for the optimal ratio of the state variables:

$$h_2^* = \left[\frac{2\big[\delta\rho c + \delta^2 c(1-\eta_1-\gamma/2)\big] + \delta^2\gamma c}{2\big[\delta\rho c + \delta^2 c(1-\eta_2-\gamma/2)\big] + \delta^2\gamma c}\right]^{\frac{1}{2-2\eta_2}} (h_1^*)^{\frac{1-\eta_1}{1-\eta_2}}. \tag{6.19}$$

Note that if $\eta_1 = \eta_2$ then (6.19) implies $h_1^* = h_2^*$. Under the maintained assumption $\eta_1 > \eta_2$ and $h_1^* > 1$, the inequalities

$$0 < \frac{2[\delta\rho c + \delta^2 c(1-\eta_1-\gamma/2)] + \delta^2\gamma c}{2[\delta\rho c + \delta^2 c(1-\eta_2-\gamma/2)] + \delta^2\gamma c} < 1, \qquad \frac{1}{2} < \frac{1}{2-2\eta_2} < 1, \qquad 0 < \frac{1-\eta_1}{1-\eta_2} < 1$$

hold, so eventually $h_2^* < h_1^*$: the optimum level of human capital for the family with lower learning ability falls short of the other family's optimum.

Using (6.19) and the steady-state costate conditions leads to a single scalar equation determining h_1^*. After algebraic manipulation one obtains the implicit equation

$$\begin{aligned} 1 = {} & \left\{ \frac{\delta\rho c + \delta^2 c(1-\eta_1-\gamma/2)}{A^2} \left[\frac{2\big[\delta\rho c + \delta^2 c(1-\eta_2-\gamma/2)\big] + \delta^2\gamma c}{2\big[\delta\rho c + \delta^2 c(1-\eta_1-\gamma/2)\big] + \delta^2\gamma c}\right]^{\frac{\gamma}{2-2\eta_2}} \right. \\ & \left. - \frac{\delta^2\gamma c}{2A^2} \left[\frac{2\big[\delta\rho c + \delta^2 c(1-\eta_1-\gamma/2)\big] + \delta^2\gamma c}{2\big[\delta\rho c + \delta^2 c(1-\eta_2-\gamma/2)\big] + \delta^2\gamma c}\right]^{\frac{2-2\eta_2-\gamma}{2-2\eta_2}} \right\} (h_1^*)^{\frac{(2-\gamma)(1-\eta_1-\eta_2)-\gamma+2\eta_1\eta_2}{1-\eta_2}} \\ & \equiv h\big(h_1^*\big), \end{aligned} \tag{6.20}$$

which uniquely determines h_1^* (see Appendix I) and, by (6.19), h_2^*. It can be shown that h_1^* positively depends on η_2 (see Appendix J). Intuitively, when learning is a social activity with interacting agents, the student with inferior learning ability can hold her fellow classmate back from fulfilling her learning potential.

Most importantly, (6.19) and (6.20) describe h_1^* and h_2^* as functions of η_1 and η_2, just as in the equilibrium case. We expect the same qualitative result to hold for the social optimum: it can be shown that each optimal knowledge level is positively influenced by both η_1 and η_2. These results align with the intuition that the planner's optimal capital stocks for both agents increase with their learning abilities.

Hence there exists a unique h_1^* and, by (6.19), a unique h_2^*; the corresponding costates θ_1^* and θ_2^* are given in closed form by (6.18a) and (6.18b). These constitute the candidate steady

state to which the system should converge under the social planner's control in the extension of the isolated-individual model. As a final step we examine whether the two-student system exhibits saddle-path stability, i.e., whether the optimum is stable in a sufficiently large neighborhood of the steady state. Because the system has two states and two costates, a purely qualitative phase-diagram analysis is not decisive; instead we linearize the system around the steady state and inspect the Jacobian.

The Jacobian of the linearized system at the steady state is

$$J \;=\; \begin{bmatrix} J_{11} & J_{12} & J_{13} & J_{14} \\ J_{21} & J_{22} & J_{23} & J_{24} \\ J_{31} & J_{32} & J_{33} & J_{34} \\ J_{41} & J_{42} & J_{43} & J_{44} \end{bmatrix}, \tag{6.21}$$

with the entries given by the partial derivatives of the right-hand sides of the state and costate equations evaluated at $(h_1^*, h_2^*, \theta_1^*, \theta_2^*)$. Explicitly,

$$J_{11} = \frac{\partial \dot{h}_1}{\partial h_1} = \frac{A^2}{c}(2\eta_1 + \gamma)\,\theta_1\, h_1^{2\eta_1+\gamma-1}\, h_2^{\gamma} - \delta, \tag{6.22}$$

$$J_{12} = \frac{\partial \dot{h}_1}{\partial h_2} = \frac{\gamma A^2}{c}\,\theta_1\, h_1^{2\eta_1+\gamma}\, h_2^{\gamma-1}, \tag{6.23}$$

$$J_{13} = \frac{\partial \dot{h}_1}{\partial \theta_1} = \frac{A^2}{c}\, h_1^{2\eta_1+\gamma}\, h_2^{\gamma}, \tag{6.24}$$

$$J_{14} = \frac{\partial \dot{h}_1}{\partial \theta_2} \;=\; 0, \tag{6.25}$$

$$J_{21} = \frac{\partial \dot{h}_2}{\partial h_1} = \frac{\gamma A^2}{c}\,\theta_2\, h_1^{\gamma-1}\, h_2^{2\eta_2+\gamma}, \tag{6.26}$$

$$J_{22} = \frac{\partial \dot{h}_2}{\partial h_2} = \frac{A^2}{c}(2\eta_2 + \gamma)\,\theta_2\, h_1^{\gamma}\, h_2^{2\eta_2+\gamma-1} - \delta, \tag{6.27}$$

$$J_{23} = \frac{\partial \dot{h}_2}{\partial \theta_1} \;=\; 0, \tag{6.28}$$

$$J_{24} = \frac{\partial \dot{h}_2}{\partial \theta_2} = \frac{A^2}{c}\, h_1^{\gamma}\, h_2^{2\eta_2+\gamma}, \tag{6.29}$$

$$J_{31} = \frac{\partial \dot{\theta}_1}{\partial h_1} = h_1^{-2} - \frac{A^2}{c}(\eta_1 + \tfrac{\gamma}{2})(2\eta_1 + \gamma - 1)\,\theta_1^2\, h_1^{2\eta_1+\gamma-2}\, h_2^{\gamma} - \frac{\gamma A^2}{2c}(\gamma - 1)\,\theta_2^2\, h_1^{\gamma-2}\, h_2^{2\eta_2+\gamma}, \tag{6.30}$$

$$J_{32} = \frac{\partial \dot{\theta}_1}{\partial h_2} = -\frac{\gamma A^2}{c}(\eta_1 + \tfrac{\gamma}{2})\,\theta_1^2\, h_1^{2\eta_1+\gamma-1}\, h_2^{\gamma-1} - \frac{\gamma A^2}{2c}(2\eta_2 + \gamma)\,\theta_2^2\, h_1^{\gamma-1}\, h_2^{2\eta_2+\gamma-1}, \tag{6.31}$$

$$J_{33} = \frac{\partial \dot{\theta}_1}{\partial \theta_1} = (\rho + \delta) - \frac{2A^2}{c}(\eta_1 + \tfrac{\gamma}{2})\,\theta_1\, h_1^{2\eta_1+\gamma-1}\, h_2^{\gamma}, \tag{6.32}$$

$$J_{34} = \frac{\partial \dot{\theta}_1}{\partial \theta_2} = -\frac{\gamma A^2}{c}\,\theta_2\, h_1^{\gamma-1}\, h_2^{2\eta_2+\gamma}, \tag{6.33}$$

$$J_{41} = \frac{\partial \dot{\theta}_2}{\partial h_1} = -\frac{\gamma A^2}{c}(\eta_2 + \tfrac{\gamma}{2})\,\theta_2^2\, h_1^{\gamma-1}\, h_2^{2\eta_2+\gamma-1} - \frac{\gamma A^2}{2c}(2\eta_1 + \gamma)\,\theta_1^2\, h_1^{2\eta_1+\gamma-1}\, h_2^{\gamma-1}, \tag{6.34}$$

$$J_{42} = \frac{\partial \dot{\theta}_2}{\partial h_2} = h_2^{-2} - \frac{A^2}{c}(\eta_2 + \tfrac{\gamma}{2})(2\eta_2 + \gamma - 1)\,\theta_2^2\, h_1^{\gamma}\, h_2^{2\eta_2+\gamma-2} - \frac{\gamma A^2}{2c}(\gamma - 1)\,\theta_1^2\, h_1^{2\eta_1+\gamma}\, h_2^{\gamma-2}, \tag{6.35}$$

$$J_{43} = \frac{\partial \dot{\theta}_2}{\partial \theta_1} = -\frac{\gamma A^2}{c}\,\theta_1\, h_1^{2\eta_1+\gamma}\, h_2^{\gamma-1}, \tag{6.36}$$

$$J_{44} = \frac{\partial \dot{\theta}_2}{\partial \theta_2} = (\rho + \delta) - \frac{2A^2}{c}(\eta_2 + \tfrac{\gamma}{2})\,\theta_2\, h_1^{\gamma}\, h_2^{2\eta_2+\gamma-1}. \tag{6.37}$$

All entries above are to be evaluated at the steady state $(h_1^*, h_2^*, \theta_1^*, \theta_2^*)$ given by (6.20), (6.19) and (6.18). The closed-form eigenvalues of J are not illuminating, so we rely on numerical exploration and parameter-region arguments. Under a wide array of normal parameter configurations the linearized system exhibits two positive and two negative eigenvalues. Consequently a saddle path exists: when the states are below their steady-state values the costates lie above their corresponding optima, and, as in the isolated case, one expects $\dot{h}_i(t) > 0$ and $\dot{\theta}_i(t) < 0$ for $i = 1, 2$. Thus, although the external effect modifies the optimum and the equilibrium, it does not destroy uniqueness of the optimum nor the saddle-path stability of the dynamics.

To complement the analytical stability results, we explore the social optimum numerically. Figure 9, along with the corresponding optimization data presented in Tables 5 and 6, reveals

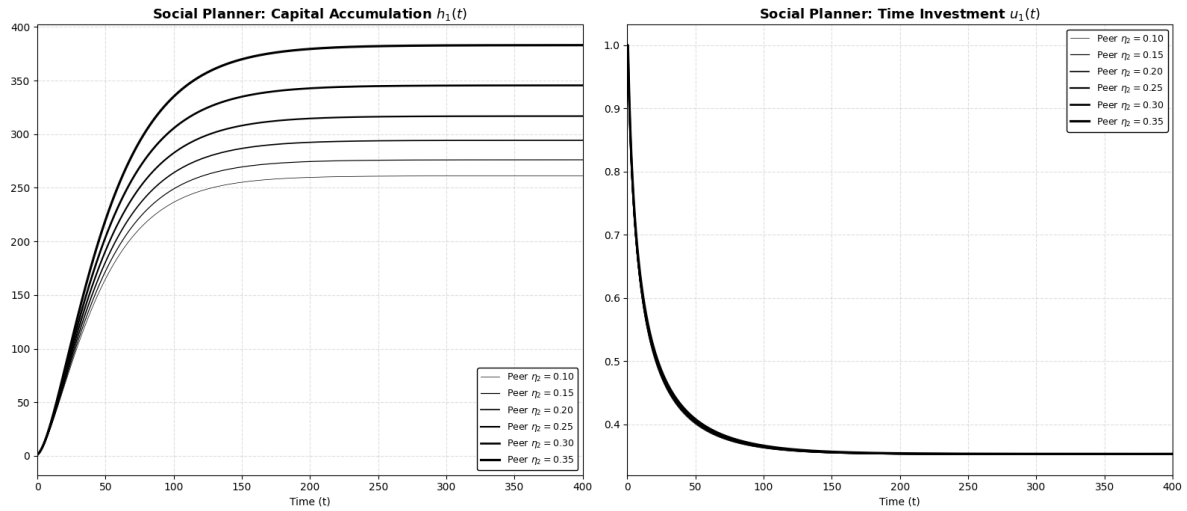


Figure 9: **Capital accumulation (left) and optimal time investment (right) for a high-ability agent ($\eta_1 = 0.45$) matched with peers of varying abilities ($\eta_2 \in [0.10, 0.40]$) in the social planner's optimum. The parameter vector is $[A, c, \delta, \gamma, \rho] = [1, 5, 0.04, 0.2, 0.05]$.**

both expected structural symmetries with the decentralized equilibrium and a fundamental divergence in early-stage incentive mechanisms.

As shown in the figure, the terminal human capital of the high-ability agent remains a strictly increasing and strictly convex function of the peer's learning ability (η_2). This confirms that the synergistic gains of peer quality persist under the social planner. Furthermore, mirroring the theoretical possibilities outlined in the isolated-individual case, both the decentralized and social optimum capital trajectories exhibit a strictly convex initial accumulation phase.

Typically, the optimal time investment $u_1(t)$ is an increasing function of η_2. However, a critical structural difference between individual selfishness and the social planner's logic emerges in the initial accumulation phase ($t = 0$). In the decentralized equilibrium, as we have seen, the high-ability agent treats the capable peer as a substitute for their own effort to alleviate capital scarcity; consequently, the shadow price in any t decreases with η_2, dragging down early time investment and allowing the agent to free-ride. Time investment becomes an increasing function of η_2 only after the peer's knowledge level is high enough to overcompensate for the negative effect of the shadow price.

The social planner perfectly avoids this early-stage waste. By internalizing the cross-agent externalities, the planner evaluates the high-ability agent's human capital not merely as a private asset, but as a crucial catalyst for the peer's growth. To prevent initial shirking, the planner reverses the decentralized early-stage shadow price pattern: as Table 5 explicitly demonstrates, in the social optimum, the initial shadow price (θ_1) becomes a strictly increasing function of η_2.

Crucially, this early-stage escalation of the shadow price is not merely a numerical artifact caused by the physical time limit $u_1(t) \leq 1$. Solving the corresponding unconstrained system confirms the exact same structural pattern. Thus, the elevated initial shadow price reflects

Table 5: **Shadow price $\theta_1(t)$ of the high-ability agent ($\eta_1 = 0.45$) paired with varying peers in the social planner's optimum. In contrast with the decentralized equilibrium, in $t = 0$, the shadow price is increasing in η_2. The parameter vector is $[A, c, \delta, \gamma, \rho] = [1, 5, 0.04, 0.2, 0.05]$.**

t	$\eta_2 = 0.10$	$\eta_2 = 0.15$	$\eta_2 = 0.20$	$\eta_2 = 0.25$	$\eta_2 = 0.30$	$\eta_2 = 0.35$
0	4.806188	4.825121	4.846820	4.871913	4.901237	4.935922
5	0.814891	0.805417	0.794992	0.783455	0.770603	0.756181
10	0.397530	0.389720	0.381137	0.371655	0.361117	0.349325
20	0.192170	0.186619	0.180550	0.173885	0.166531	0.158376
50	0.088200	0.084535	0.080559	0.076235	0.071522	0.066373
100	0.064578	0.061394	0.057949	0.054217	0.050172	0.045788
200	0.059509	0.056379	0.052987	0.049309	0.045319	0.040994
300	0.059242	0.056108	0.052711	0.049025	0.045023	0.040682
400	0.059229	0.056095	0.052697	0.049010	0.045007	0.040664

Table 6: **High-Ability Agent ($\eta_1 = 0.45$) optimal time investment $u_1(t)$ paired with varying peers in the social planner's optimum. The parameter vector is $[A, c, \delta, \gamma, \rho] = [1, 5, 0.04, 0.2, 0.05]$.**

t	$\eta_2 = 0.10$	$\eta_2 = 0.15$	$\eta_2 = 0.20$	$\eta_2 = 0.25$	$\eta_2 = 0.30$	$\eta_2 = 0.35$
0	1.000000	1.000000	1.000000	1.000000	1.000000	1.000000
50	0.400183	0.401319	0.402613	0.404103	0.405836	0.407879
100	0.362094	0.362655	0.363296	0.364039	0.364911	0.365950
150	0.354173	0.354504	0.354876	0.355297	0.355784	0.356358
200	0.352337	0.352589	0.352862	0.353161	0.353494	0.353872
250	0.351903	0.352130	0.352372	0.352630	0.352908	0.353212
300	0.351800	0.352020	0.352252	0.352498	0.352758	0.353037
350	0.351776	0.351994	0.352223	0.352465	0.352720	0.352991
400	0.351785	0.352004	0.352235	0.352479	0.352738	0.353015

the planner's pure economic valuation of the synergistic potential, mathematically coercing the high-ability agent into exerting maximal effort from the very beginning to properly ignite the growth engine.

7 Comparative dynamics

As we have seen above, learning in a social setting affects the learning parameters A and η of the isolated case. To trace back to the isolated case how individuals behave in a social environment, we need to understand how changes in A (taken as $Ah_i^{\gamma/2}$ in the learning function for each agent) and η change the behavior of the isolated system. The former change comes from the increase of the capital stock of the fellow classmate, while the latter stems from how the external effect elevates the learning parameters η_i, $i = 1, 2$. The endpoints of convergence in the isolated case are pinned down by h^* and θ^*, the behavior of

which is revealed by the partial differentials of the optimum solutions of the isolated case. However, these results are informative about the endpoints of convergence only. To see how the optimal trajectories change in the equilibrium and the optimum of the social case, we need to examine the comparative dynamics of the isolated case. Therefore, we still reduce the dynamics of the social setting to the case of the isolated individual as much as possible. To do so, we combine Oniki's (1973) and Caputo's (1990b) phase-diagram approach with Caputo's (1990a; 2005, pp. 287–311) dynamic envelope theorem.

The qualitative phase-diagram approach is built on the idea that a change in a parameter modifies $\dot{h}$ and $\dot{\theta}$ through changing the paths of h and θ as well as, with given h_0, the starting value $\theta(0)$ along the saddle path. Most of the work is to find the starting points and endpoints of the perturbed system. We can skip some of these steps because, with given h_0, isoquant analysis yields $\partial\theta(0)/\partial\eta > 0$ and $\partial\theta(0)/\partial A < 0$, and it indicates how changes in η and A affect the endpoints h^* and θ^* (note that the sign of $\partial\theta^*/\partial\eta$ is uncertain). Thus the only step required to draw the phase diagrams is to differentiate the system of laws of motion for h and θ in (3.10) and (3.11) with respect to η and A (see Appendix A). Differentiation with respect to η yields the following linearized system for the comparative dynamics:

$$\frac{\partial\dot{h}}{\partial\eta} = \frac{A^2}{c}\,h^{2\eta}\,\frac{\partial\theta}{\partial\eta} + \left(\frac{2\eta A^2}{c}\,\theta\,h^{2\eta-1} - \delta\right)\frac{\partial h}{\partial\eta} + \frac{2A^2}{c}\,\theta\,h^{2\eta}\ln h, \tag{7.1a}$$

$$\begin{aligned}\frac{\partial\dot{\theta}}{\partial\eta} = {}& \left[(\rho+\delta) - \frac{2\eta A^2}{c}\,\theta\,h^{2\eta-1}\right]\frac{\partial\theta}{\partial\eta} + \left[h^{-2} + \frac{\eta A^2}{c}(1-2\eta)\,\theta^2\,h^{2\eta-2}\right]\frac{\partial h}{\partial\eta} \\ & - \frac{A^2}{c}\,\theta^2\,h^{2\eta-1} - \frac{\eta A^2}{c}\,\theta^2\big(2h^{2\eta-1}\ln h\big).\end{aligned} \tag{7.1b}$$

This system can be written in compact matrix form as

$$\begin{pmatrix}\partial\dot{\theta}/\partial\eta \\ \partial\dot{h}/\partial\eta\end{pmatrix} = \begin{pmatrix}+ & - \\ + & +\end{pmatrix}\begin{pmatrix}\partial\theta/\partial\eta \\ \partial h/\partial\eta\end{pmatrix} + \begin{pmatrix}- \\ +\end{pmatrix}, \tag{7.2}$$

where the entries of the 2×2 coefficient matrix and the inhomogeneous vector are given by the coefficients in (7.1). The phase diagram in Fig. 10 follows.

As $\partial\theta(0)/\partial\eta > 0$ and with a given h_0, after an increase in η the perturbed process starts somewhere on the positive segment of the vertical axis from which no route leads to the left. As we expect $\partial h^*/\partial\eta > 0$ while $\partial\theta^*/\partial\eta$ is uncertain, the endpoints of the perturbed convergences must lie in the positive half of the plane lying to the right of the vertical axis. Paths A and B in Fig (10) are such typical cases. From the starting points, we move to the right, which means that an increase in η elevates the whole capital profile, so the change leads to higher capital stocks at any t. However, based on the directions of flows, we cannot exclude a case such as path C, a part of which lies to the left of the vertical axis, meaning that while $\dot{h} > 0$ holds all along, an increase in η lowers the capital profile and slows the speed of the accumulation of the capital stock for a while. In such a case, the continuously increasing capital profile with a higher η is temporarily under the capital profile implied by a lower η. We shall return to this case below.

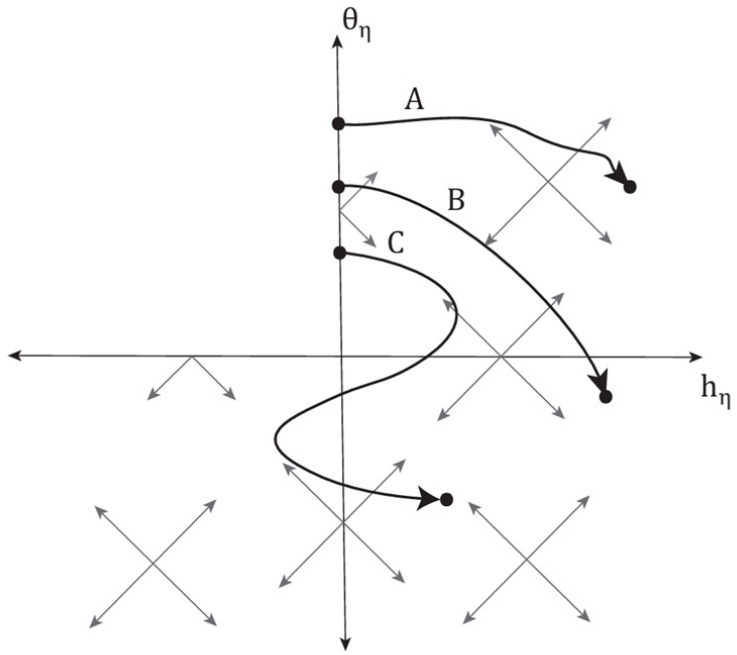


Figure 10: **Phase diagram of the convergence perturbed by an increase in η.**

The differentiation with respect to A yields the equations

$$\frac{\partial \dot{h}}{\partial A} = \frac{A^2}{c}\, h^{2\eta}\, \frac{\partial \theta}{\partial A} + \left(\frac{2\eta A^2}{c}\, \theta\, h^{2\eta-1} - \delta \right) \frac{\partial h}{\partial A} + \frac{2A}{c}\, \theta\, h^{2\eta}, \tag{7.3a}$$

$$\frac{\partial \dot{\theta}}{\partial A} = \left[(\rho + \delta) - \frac{2\eta A^2}{c}\, \theta\, h^{2\eta-1} \right] \frac{\partial \theta}{\partial A} + \left[h^{-2} + \frac{\eta A^2}{c} (1 - 2\eta)\, \theta^2\, h^{2\eta-2} \right] \frac{\partial h}{\partial A} - \frac{2\eta A}{c}\, \theta^2\, h^{2\eta-1}. \tag{7.3b}$$

This takes the general form

$$\begin{bmatrix} \partial \dot{\theta}/\partial A \\ \partial \dot{h}/\partial A \end{bmatrix} = \begin{bmatrix} +/- & + \\ + & +/- \end{bmatrix} \begin{bmatrix} \partial \theta/\partial A \\ \partial h/\partial A \end{bmatrix} + \begin{bmatrix} - \\ + \end{bmatrix},$$

from which the phase diagram in Fig. (11) follows.

As $\partial \theta(0)/\partial A < 0$ and with a given h_0, after an increase in A the perturbed process starts somewhere on the negative segment of the vertical axis from which routes do lead to the left as well. It is also known that $\partial h^*/\partial A > 0$ and $\partial \theta^*/\partial A < 0$, so the endpoints certainly lie in the bottom-right quadrant. Path A is a typical case where the whole convergence process runs to the right of the vertical axis, meaning that an increase in A elevates the whole capital profile. In this case, a higher A, other things equal, implies a higher capital stock at any $t > 0$ (note that h_0 is fixed). However, just like in the perturbation analysis of η, a case like path B cannot be ruled out, so it might happen that an increase in A temporarily reduces the speed of capital accumulation. In such a case, while $\dot{h} > 0$ holds throughout

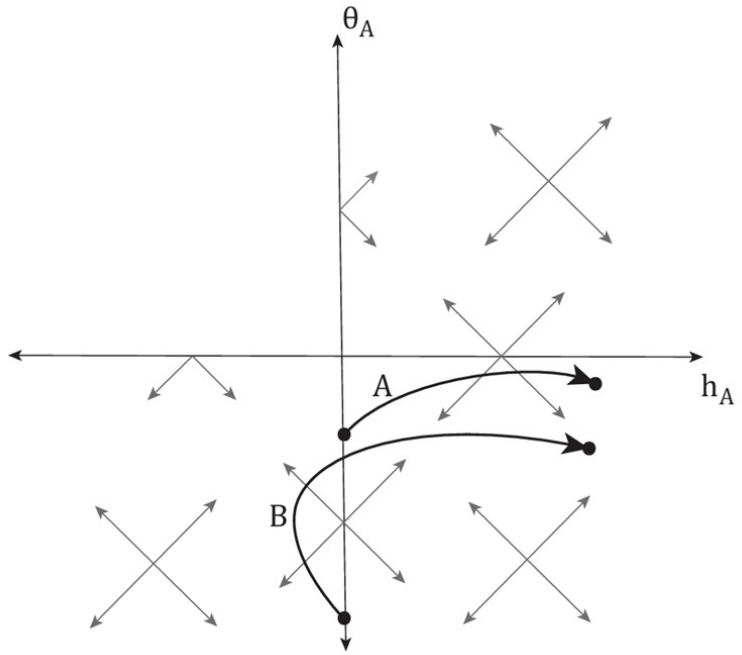


Figure 11: **Phase diagram of the convergence perturbed by an increase in A.**

the accumulation process, an initial segment of the capital profile implied by a higher A lies below the capital path implied by a lower A.

These results can be revisited and sharpened by Caputo's envelope-theorem framework. As there is a constraint on the control given as $0 \leq u(t) \leq 1$, the Lagrangian of the isolated case is simply

$$\mathcal{L} = \ln(h) - \frac{c}{2}u^2 + \theta\big(Ah^{\eta}u - \delta h\big) + \mu(u-1),$$

in which μ is the Kuhn–Tucker multiplier corresponding to the control variable. The dynamic envelope theorem results come from differentiating $\mathcal{L}$ with respect to the relevant parameters, now η and A, then evaluating and integrating the expression along the optimal paths $h^*(t,\beta)$, $\theta^*(t,\beta)$ and $u^*(t,\beta)$. As the Kuhn–Tucker part does not depend on either η or A, we may simply differentiate the Hamiltonian. The results

$$\frac{\partial \mathcal{L}}{\partial A} = \theta h^{\eta}u, \qquad \left.\frac{\partial \mathcal{L}}{\partial A}\right|_{\text{optimal}} = \theta^*(t,\beta)\,[h^*(t,\beta)]^{\eta}\,u^*(t,\beta),$$

and

$$J_A^*(\beta) = \int_0^{\infty} \theta^*(t,\beta)\,[h^*(t,\beta)]^{\eta}\,u^*(t,\beta)\,dt > 0 \tag{7.4}$$

follow, in which the parameter vector β contains not only A, c, η, δ, but also h_0. Given that $1 < h_0 < h^*$ by assumption, the analogous result with respect to η is

$$J_{\eta}^*(\beta) = A\int_0^{\infty} \theta^*(t,\beta)\,[h^*(t,\beta)]^{\eta}\ln\big[h^*(t,\beta)\big]\,u^*(t,\beta)\,dt > 0, \tag{7.5}$$

according to which a rise in either η or A increases the value obtained under optimal behavior.

In the next step, (7.4) and (7.5) are to be differentiated with respect to η and A, which yields

$$H_{11} \equiv J^*_{AA}(\beta) = \int_0^\infty \frac{\partial}{\partial A}\theta^*(t,\beta)\,[h^*(t,\beta)]^\eta\,u^*(t,\beta)\,dt = 0,$$

$$H_{22} \equiv J^*_{\eta\eta}(\beta) = A\int_0^\infty \frac{\partial}{\partial \eta}\theta^*(t,\beta)\,[h^*(t,\beta)]^\eta \ln\big[h^*(t,\beta)\big]\,u^*(t,\beta)\,dt$$

$$= A\int_0^\infty \theta^*(t,\beta)\,[h^*(t,\beta)]^\eta \big(\ln[h^*(t,\beta)]\big)^2 u^*(t,\beta)\,dt > 0,$$

and

$$H_{12} = H_{21} \equiv J^*_{A\eta}(\beta) = \int_0^\infty \frac{\partial}{\partial \eta}\theta^*(t,\beta)\,[h^*(t,\beta)]^\eta\,u^*(t,\beta)\,dt$$

$$= \int_0^\infty \theta^*(t,\beta)\,[h^*(t,\beta)]^\eta \ln\big[h^*(t,\beta)\big]\,u^*(t,\beta)\,dt = J^*_{\eta A}(\beta) > 0.$$

These entries can be summarized in the Hessian

$$H = \begin{bmatrix} H_{11} & H_{12} \\ H_{21} & H_{22} \end{bmatrix} = \begin{bmatrix} 0 & + \\ + & + \end{bmatrix}.$$

Given this structure, $\det(H) < 0$. Since the determinant equals the product of the eigenvalues and both eigenvalues are real, the eigenvalues have opposite signs (Horn & Johnson, 2013, pp. 50–51). Using standard results on definiteness (Horn & Johnson, 2013, p. 430), the mixed signs imply that H is indefinite.[4]

Note, however, that when η is treated on its own, judged by the positive sign in the $(2,2)$ position of H, the one-element Hessian $H_{22} \in \mathbb{R}^{1\times 1}$ is positive definite. Therefore, as the integral in (7.5) is strictly positive, a marginal rise in η increases the value of the optimal behavior and, through the optimality conditions, results in a higher optimal capital profile $h^*(t,\beta)$ starting from any $1 < h_0 < h^*$ under any appropriate parameter configurations, for all $t > 0$ and with no change in other parameters. Consequently, $J^*(\beta)$ is a strictly increasing

[4]If we treat all the four parameters A, η, c, and δ, the Hessian

$$\hat{H} = \begin{bmatrix} 0 & + & 0 & 0 \\ + & + & 0 & 0 \\ 0 & 0 & 0 & 0 \\ 0 & 0 & 0 & 0 \end{bmatrix}$$

is still indefinite. To see this, we just need to use the fact that $\hat{H}$ is a block diagonal matrix, and the eigenvalues of $\hat{H}$ are the eigenvalues of the top left and bottom right blocks, the bottom left and top right blocks being zero. While the bottom right block has two zero eigenvalues, the top left block has just proven to be indefinite. In Caputo's framework, the direction of the effect of a parameter change is determined by the integrated differential of the Lagrangian. To have clear results, the Hessian must be either positive or negative definite or semi-definite.

and locally strictly convex function of η, so the effect of η on the state profile may even be accelerated by further marginal increases; these effects are not expected to fade away. This result rules out path C in Fig. (10).

We have a similar result for A. As the integral in (7.4) is strictly positive, a marginal rise in A increases the value of the optimal behavior, and, through the optimality conditions, results in a higher optimal capital profile $h^*(t, \beta)$ starting from any $1 < h_0 < h^*$ under any appropriate parameter configuration, for all $t > 0$ and all other parameters kept fixed, as the Hessian $H_{11} \in \mathbb{R}^{1\times1}$ of A is zero, hence semidefinite. Consequently, $J^*(\beta)$ is a strictly increasing and linear function of A. This result excludes path B in Fig. (11).

The fact that H is indefinite implies that $J^*(\beta)$ is neither a strictly convex nor a strictly concave function of the parameters η and A. Therefore, there might be some direction in the two-dimensional parameter space $\eta \times A \subset \mathbb{R}^2$ along which increasing η and A simultaneously might lead to ambiguous or even counteracting effects on the capital profile of the isolated individual. It means that when increasing η and A simultaneously under a parameter configuration, the atypical behavior of a temporary capital-profile drop might occur. In this case, given any $h(t)$, keeping $\dot{h}$ above zero is possible with lower $u(t)$, so the atypical case is straightforward to interpret as saving learning time due to higher productivity in learning.

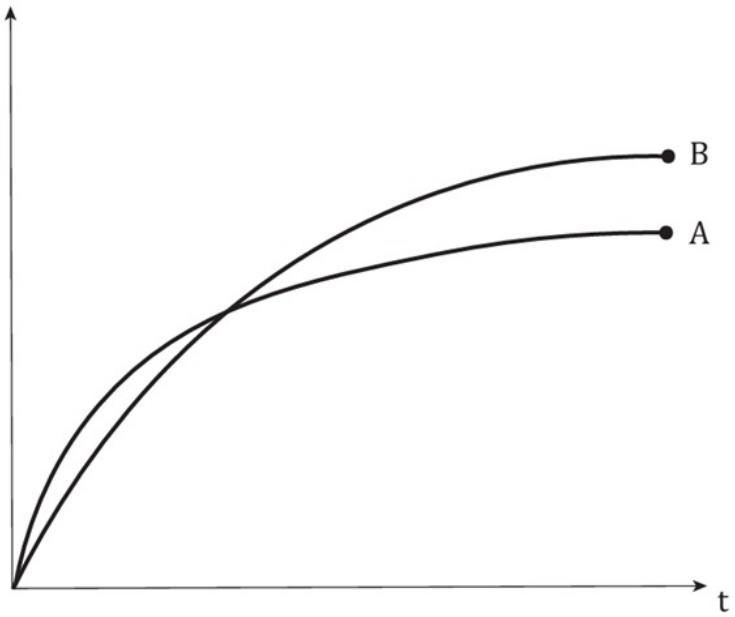


Figure 12: **A schematic representation of the atypical behavior of saving learning time in the isolated case. The baseline case is A, while the path running toward B takes place after a simultaneous increase in η and A.**

When applying these results to the equilibrium allocation and paths, however, we must take into account the fact that the parameter $\eta_i + \gamma/2$ is fixed for both agents ($i = 1, 2$) throughout the capital-accumulation process. Therefore, simultaneous changes in $\eta_i + \gamma/2$ and A taken as changes in $Ah_j^{\gamma/2}$ are excluded; only $Ah_j^{\gamma/2}$ increases over time as $h_j(t)$ increases in time ($j = 1, 2$). This change, however, can easily be traced back to changes in

A of the isolated case above.

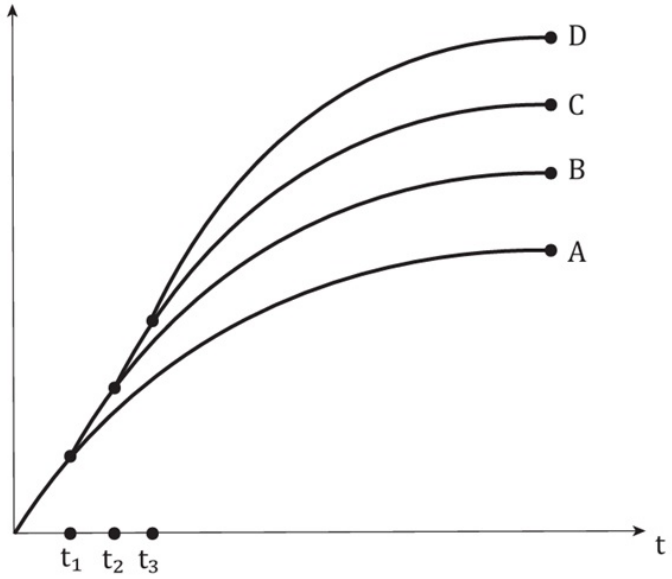


Figure 13: **A schematic representation of the capital profile of the individual in the equilibrium setting. The actual path is the upper-envelope curve of the series of paths. The temporary endpoints A, B, C and D are continuously updated and increasing as the capital stock of the fellow classmate increases. This continuous update is approximated with discrete-time updates taking place at t_1, t_2 and t_3.**

In every moment, the increase in the capital stock of the fellow classmate opens a new capital path for the individual in the equilibrium setting that she experiences as an exogenous increase in parameter A in the learning function. Under any appropriate parameter configuration, a part of which is the capital stock of the fellow classmate, there is a stable manifold along which $\dot{h}_i > 0$ holds. The saddle-path property seen above guarantees local uniqueness and convergence at every moment and at any capital distribution in the setting. The increase in the capital stock of the fellow classmate at any moment leads to a higher capital path in line with how the endpoints of capital convergence are increasing. Given the results from comparative dynamics above, to our previous insights we can add the additional finding that to any temporary endpoint of capital convergence (points A, B, C and D in Fig. (13) there belongs a unique capital path for each agent that is above all the capital paths belonging to any previous temporary endpoints.

These results are easy to extend to the optimum of the social setting defined in (6.2a), (6.2b), and (6.16). In this two-state and two-costate case we cannot use the phase-diagram approach, so we must start out with the application of the dynamic envelope theorem. The Lagrangian of the problem is

$$\widetilde{\mathcal{L}} = \widetilde{H}(h_1, h_2, \theta_1, \theta_2, u_1, u_2) =$$
$$\ln h_1 + \ln h_2 - \frac{c}{2}u_1^2 - \frac{c}{2}u_2^2 + \theta_1\big(Ah_2^{\gamma/2}h_1^{\eta_1+\gamma/2}u_1 - \delta h_1\big)$$
$$+ \theta_2\big(Ah_1^{\gamma/2}h_2^{\eta_2+\gamma/2}u_2 - \delta h_2\big) + \mu_1(u_1 - 1) + \mu_2(u_2 - 1). \tag{7.6}$$

The direct differentiation of $\widetilde{\mathcal{L}}$ with respect to A yields

$$\frac{\partial \widetilde{\mathcal{L}}}{\partial A} = \theta_1\, h_2^{\gamma/2}\, h_1^{\eta_1+\gamma/2}\, u_1 + \theta_2\, h_1^{\gamma/2}\, h_2^{\eta_2+\gamma/2}\, u_2,$$

from which integration along the optimum paths leads to

$$\widetilde{J}_A^*(\beta) = \int_0^\infty \Big[\theta_1^*(t,\beta)\, h_2^*(t,\beta)^{\gamma/2}\, h_1^*(t,\beta)^{\eta_1+\gamma/2}\, u_1^*(t,\beta)$$
$$+ \theta_2^*(t,\beta)\, h_1^*(t,\beta)^{\gamma/2}\, h_2^*(t,\beta)^{\eta_2+\gamma/2}\, u_2^*(t,\beta)\Big]\, dt > 0. \tag{7.7}$$

Of the other two partial differentials, the first is

$$\frac{\partial \widetilde{\mathcal{L}}}{\partial \eta_1} = \theta_1\, A\, h_2^{\gamma/2}\, h_1^{\eta_1+\gamma/2}\, \ln(h_1)\, u_1,$$

from which the integral along the optimum paths

$$\widetilde{J}_{\eta_1}^*(\beta) > 0$$

is certainly positive as long as the starting value $h_1(0) > 1$ holds by assumption (analogous to the isolated case). By symmetry,

$$\widetilde{J}_{\eta_2}^*(\beta) > 0$$

also follows. Using the linearity of $\widetilde{J}^*(\beta)$ in parameter A, the upper-left element in the Hessian $\widetilde{H}$ of the problem is $\widetilde{H}_{11} \equiv \widetilde{J}_{AA}^*(\beta) = 0$.

Most importantly,

$$\widetilde{H}_{22} \equiv \widetilde{J}_{\eta_1\eta_1}^*(\beta) = A\int_0^\infty \frac{\partial}{\partial \eta_1}\Big[\theta_1^*(t,\beta)\, h_2^*(t,\beta)^{\gamma/2}\, h_1^*(t,\beta)^{\eta_1+\gamma/2}\, \ln\big(h_1^*(t,\beta)\big)\, u_1^*(t,\beta)\Big]\, dt$$

$$= A\int_0^\infty \theta_1^*(t,\beta)\, h_2^*(t,\beta)^{\gamma/2}\, h_1^*(t,\beta)^{\eta_1+\gamma/2}\big(\ln h_1^*(t,\beta)\big)^2\, u_1^*(t,\beta)\, dt > 0,$$

under the previous assumption regarding the starting value for $h_1(t)$. By symmetry,

$$\widetilde{H}_{33} \equiv \widetilde{J}_{\eta_2\eta_2}^*(\beta) > 0$$

also holds.

Regarding the off-diagonal elements of $\widetilde{H}$,

$$\widetilde{H}_{12} = \widetilde{H}_{21} \equiv \widetilde{J}^*_{A\eta_1}(\beta) = \int_0^\infty \theta_1^*(t,\beta)\, h_2^*(t,\beta)^{\gamma/2}\, h_1^*(t,\beta)^{\eta_1+\gamma/2}\, \ln\big(h_1^*(t,\beta)\big)\, u_1^*(t,\beta)\, dt > 0,$$

and symmetry implies $\widetilde{H}_{13} = \widetilde{H}_{31} \equiv \widetilde{J}^*_{A\eta_2}(\beta) > 0$. From $\partial\widetilde{\mathcal{L}}/\partial\eta_1$ and $\partial\widetilde{\mathcal{L}}/\partial\eta_2$ it follows that

$$\widetilde{H}_{23} = \widetilde{H}_{32} \equiv \widetilde{J}^*_{\eta_1\eta_2}(\beta) = 0.$$

From this analysis, the Hessian in its general form is

$$\widetilde{H} = \begin{bmatrix} 0 & + & + \\ + & + & 0 \\ + & 0 & + \end{bmatrix},$$

which is again indefinite (see Appendix K). Accordingly, as in the equilibrium setting, there is a direction in the parameter space $(\eta_1, \eta_2, A) \subset \mathbb{R}^3$ along which increasing η_1, η_2 and A simultaneously might lead to ambiguous or even counteracting effects on the capital profile of the isolated individual.

However, it still holds that the parameter $\eta_i + \gamma/2$ is fixed for each individual $(i = 1, 2)$ throughout the capital-accumulation process. Therefore, only $Ah_i^{\gamma/2}$ is increasing in time as $h_i(t)$ increases in time $(i = 1, 2)$; we thus obtain the optimized dynamics of the paths depicted in Fig. (13).

8 Discussion: Rational segregation in a model of school learning

The dynamic envelope theorem results in (7.4) and (7.5) are easy to interpret as a drive for Agent 1 to select as high a parameter value for η_2 as possible. By itself, (7.5) shows that the way the agent's utility depends on η makes her interested in learning in a classroom environment instead of learning in isolation. The external effect of classroom learning adds to η. Beyond this interest, however, the actual benefit a student can realize from learning as a social activity crucially depends on the parameter η of her fellow classmate. In the equilibrium setting, therefore, selecting a classroom environment boils down to selecting a parameter η_i of a possible classmate. Assuming $\eta_1 > \eta_2$, Agent 1 realizes that higher values for η_2 imply higher capital profiles for both agents. Given the starting values of the capital stocks, both agents in a classroom setting start converging toward their temporary endpoints, which are continuously increasing as their capital stocks are continuously increasing. Agent 1, as a utility maximizer, knows, however, that a higher η_2 leads to higher $h_2(t)$ at any $t > 0$, which also boosts her own capital accumulation process through (6.3a) and (6.3b). As overall discounted utility is an increasing function of A in the equilibrium setting (by (7.4), a higher capital profile of Agent 2 makes Agent 1 happier and more satisfied, so Agent

1 is interested in finding a classmate with η_2 as close to η_1 as possible and, equivalently, in avoiding agents with low η_2 values. The rational individual having high learning ability thus tends to segregate. The case is the exact opposite for Agent 2. The way her utility depends on η_1 of a possible classmate having higher learning abilities makes her interested in finding a classmate with a learning parameter as high as possible, which makes her interested in avoiding segregation. So, based on our previous results, we can claim the following theorem. As we can use all the previous results, we do not need a formal demonstration at this point.

Theorem 1: The asymmetric drive of the individual for segregation. Assuming $\eta_1 > \eta_2$, both Student 1 and Student 2 are interested in finding a classmate with the highest possible learning parameter η_2 and η_1, respectively.

Proof. Following from $\partial h_1^e/\partial \eta_1 > 0$ and $\partial h_1^e/\partial \eta_2 > 0$ we know how h_1^e and h_2^e depend on η_1 and η_2, yielding the result that each agent's utility is an increasing function of the classmate's learning parameter η_i (Propositions 6 and 7, Appendix G). So, we only need to show that:

1. A higher learning parameter η_i of the classmate elevates the entire capital profile of the agent, and

2. The rational utility-maximizing agent prefers a higher capital profile; therefore, she prefers a classmate having a higher learning parameter η_i to a classmate with a lower parameter value.

As for (1), due to the external effect, the classmate's continuously increasing capital stock continuously increases the effective A for the agent, as shown in Fig. 13, placing the agent on a higher capital profile at every moment. This part of the issue has already been resolved by the perturbation analysis in Section 7. However, a missing point is how the classmate's η_i impacts this process. The same perturbation analysis showed that a higher η_i elevates the entire own capital profile. From this, in the equilibrium setting it follows that at any t (with $t > t_0$) the classmate, thanks to her higher η_i, proceeds on a higher capital profile compared to any case with a lower η_i. This higher profile affects the agent's productivity at t through increasing the effect of her A in the learning function, which leads to a higher capital profile as shown in Section 7. We also note that, thanks to her higher η_i, the classmate was on a higher capital profile at earlier times compared to the profile she would have had with a lower learning parameter. Therefore, the classmate's higher η_i elevates her entire capital profile and increases the effect of A in the learning function of the agent along her whole accumulation process. As a higher A elevates the entire capital profile for the agent, a higher η_i elevates the capital profiles for both agents in the equilibrium setting.

As for (2), given that the individual perceives the classmate's capital profile through the external effect affecting A, the question is whether the utility-maximizing individual is interested in a learning function with an increased A. Section 7 shows that a higher A increases the value of the optimal behavior; therefore, the individual is interested in having a higher A and, equivalently, in learning with a classmate who, thanks to her higher η_i, facilitates a higher A. As this holds for both agents in the equilibrium setting with $\eta_1 > \eta_2$, Agent 1 has a tendency to segregate and avoid any classmate with low η_2. By contrast, Agent 2 can maximize her utility by learning with a classmate having η_1 as high as possible, so Agent 2 is against segregation. □

We have a similar result in the optimum setting where time investments and capital paths are allocated by the social planner. To say something intelligent about the social planner's drive to segregate, however, we need to specify a mechanism for student selection. It makes a difference if the social planner maximizes total utility of the class with a given η_1 or η_2.

Theorem 2: The asymmetric drive of the social planner for segregation. Assuming $\eta_1 > \eta_2$, given η_i, the social planner is interested in finding a classmate with the highest possible learning parameter η_j, $i \neq j$.

Proof. As we have seen above, $\widetilde{L}$ is an increasing function of η_1 and η_2. Still assuming $\eta_1 > \eta_2$ and with given η_1, the Hessian $\widetilde{H}$ implies that the social planner can increase the overall utility of the class by selecting a classmate with parameter η_2 as close to η_1 as possible. In the opposite case, i.e. with given η_2, to maximize total utility the social planner picks a classmate with the highest possible η_1, which is a drive for setting up a heterogeneous class.

This choice, at the end of the day, is the maximization of the maximum utility by an optimum choice of parameters. In both the equilibrium and the optimum settings, segregation is motivated by the idea that by selecting an appropriate classmate both the individual and the social planner can influence the parameters of human capital accumulation. In Theorem 2, we assumed that student selection is a process in which the social planner treats η_1 or η_2 as given, and his task is to find an appropriate classmate—this is what was regarded above as a mechanism of student selection. □

The model as it stands now aligns with a number of empirical facts. At the most basic level, the model suggests that, other things equal, children from deprived families, hence having low η_2 due to the lack of adequate home facilities and support, naturally perform worse. As we have seen, a student with inferior learning abilities can benefit from a heterogeneous or unsegregated class environment the most when she is mixed with one having very high η_1. Accordingly, the higher the difference between η_1 and η_2 while $\eta_1 > \eta_2$ holds, the more benefit is realized by Agent 2 in the form of an increase in the equilibrium or optimum capital stock and in the elevation of the capital path. Similarly, top students benefit the most from the presence of similar students: the smaller the difference between η_1 and η_2 while $\eta_1 > \eta_2$ holds, the more benefit is realized by Agent 1 in the form of an increase in the equilibrium or optimum capital stock and in the elevation of the capital path. The external effect in the model is asymmetric—the same heterogeneous setting is harmful to the agent with high η_1 and beneficial to the agent with low η_2. The model thus predicts diverse responses to desegregation. Given that the model, other things equal, associates higher stocks of human capital to higher values of parameter η, it is straightforward to translate the implications of differences in η_i into differences in the levels of human capital. On this showing, the implications are consistent with results by, for instance, Hoxby and Weingarth (2005), who found that students with low scores benefit the most from the addition of students from the top 15% of the score distribution. Likewise, top students benefit the most from the presence of students from their own league. Imberman, Kugler, and Sacerdote (2009) also found that high-achieving students' school performance benefits the most from the presence or appearance of other high-achieving students. Lavy, Silva, and Weinhardt (2012) report that all capability cohorts of students are harmed by the presence of the lowest-achieving classmates.

The model also offers a theoretical explanation for why desegregation might fail. Desegregation efforts without strategies to improve the underlying factors—such as home environments, facilities for early-childhood learning, and family income, hence to increase η_2—might not work. In such a case, desegregation means that previously established peer networks are destroyed, so in a new, integrated environment a family with superior learning abilities is exposed to negative external effects delivered by families in low socio-economic status. This case aligns with the model's predictions according to which such a desegregation strategy is harmful to the family with high η_1 and ultimately leads to efforts to resegregate (Orfield & Lee, 2007), as low school performance in the model is not simply a consequence of segregation but can actively drive it. In this negative case, as the model predicts, students from disadvantaged backgrounds might find themselves on a downward spiral—low socioeconomic status implies poor home learning facilities that, in turn, hinder adequate progress in school, which, in turn, intensifies segregation and resegregation. The benefits a family can realize with an increased η_2 are higher, and policy measures increasing the parameter also dampen efforts to resegregate.

Appendix A

Proposition 1: The problem defined by (3.4) and (3.5) has a unique optimum steady-state solution h^* to which there belongs an optimal value θ^* for the costate variable. These solutions are finite at any configuration of appropriate and finite parameters.

Proof. To find the steady-state values, note that the point (h^*, θ^*) in the space $S = (h, \theta)$ is pinned down by the intersection of the nullclines $\dot{h} = 0$ and $\dot{\theta} = 0$. By substituting $u = A/(c)\,\theta h^{\eta}$ from (3.9) into (3.11), the latter becomes

$$\dot{h} = \frac{A^2}{c}\,\theta h^{2\eta} - \delta h \tag{A.1}$$

which, when $\dot{h} = 0$, leads to

$$\theta = \frac{\delta c}{A^2}\,h^{\,1-2\eta} \tag{A.2}$$

as the nullcline of h. Note that the shape of (A.2) depends on the value of the parameter η: for $0 < \eta < 0.5$ it is strictly increasing, while for $0.5 < \eta < 1$ it is strictly decreasing.

Finding the $\dot{\theta} = 0$ nullcline starts with the same substitution from (3.9) into (3.10), which becomes

$$\dot{\theta} = \theta\Big(\rho + \delta - \frac{A^2\eta}{c}\,\theta h^{2\eta-1}\Big) - \frac{1}{h} \tag{A.3}$$

and, when $\dot{\theta} = 0$, gives

$$\rho + \delta = \frac{1}{\theta h} + \frac{A^2\eta}{c}\,\theta h^{2\eta-1} \tag{A.4}$$

as the nullcline of θ.

Equations (A.2) and (A.4) together imply that

$$\theta^* = \frac{\delta c}{A^2} \left(h^*\right)^{1-2\eta} \tag{A.5}$$

and

$$\rho + \delta = \frac{1}{\theta^* h^*} + \frac{A^2 \eta}{c} \theta^* (h^*)^{2\eta - 1}. \tag{A.6}$$

Substituting (A.5) into (A.6) yields

$$h^* = \left(\frac{A^2/(\delta c)}{\rho + \delta(1-\eta)} \right)^{1/(2-2\eta)} > 0 \tag{A.7}$$

according to which the steady-state value h^* exists and is unique. For the other coordinate of the steady state we have

$$\theta^* = \frac{\delta c}{A^2} \left(\frac{A^2/(\delta c)}{\rho + \delta(1-\eta)} \right)^{(1-2\eta)/(2-2\eta)} > 0,$$

which exists and is unique as long as $\eta \neq 0.5$. With both h^* and θ^* finite, the transversality conditions

$$\lim_{t \to \infty} e^{-\rho t} \theta(t) \geq 0 \qquad \text{and} \qquad \lim_{t \to \infty} e^{-\rho t} \theta(t) h(t) = 0$$

obviously hold. □

Appendix B

Note that (3.9) and (3.10) imply the equation

$$\frac{A^2 \eta}{c} h^{2\eta} \theta^2 - (\rho + \delta) h \theta + 1 = 0 = \dot{\theta} \tag{B.1}$$

which defines the roots of a quadratic polynomial in θ. In the $S = (h, \theta)$ space the $\dot{\theta} = 0$ nullcline is where we find those points that satisfy (B.1). Depending on h, equation (B.1) might have zero, one or two real roots. With simple algebra we obtain the roots as

$$\frac{(\rho + \delta) h \pm \sqrt{(\rho + \delta)^2 h^2 - 4 \left(A^2 \eta / c\right) h^{2\eta}}}{2 \left(A^2 \eta / c\right) h^{2\eta}}. \tag{B.2}$$

Equations (B.1) and (B.2) define a horizontally positioned and distorted parabolic curve whose vertex is above a stock $\tilde{h} > 0$ where the radicand is zero. This condition is easy to translate into a unique capital stock

$$\tilde{h} = \left(\frac{4 \left(A^2 \eta / c\right)}{(\rho + \delta)^2} \right)^{1/(2-2\eta)} > 0.$$

It is also easy to see that the radicand is strictly increasing in h if

$$h > \left(\frac{4\,(A^2\eta^2/c)}{(\rho+\delta)^2} \right)^{1/(2-2\eta)},$$

in which the lower bound for any $0 < \eta < 1$ is strictly lower than $\tilde{h}$. Therefore, in our relevant range $\tilde{h} \leq h \leq \bar{h}$, the radicand in (B.2) is strictly increasing. From (B.2) we thus have the pair of equations

$$\begin{aligned} \theta_1(h) &= \frac{(\rho+\delta)h + \sqrt{(\rho+\delta)^2h^2 - 4\,(A^2\eta/c)\,h^{2\eta}}}{2\,(A^2\eta/c)\,h^{2\eta}}, \\ \theta_2(h) &= \frac{(\rho+\delta)h - \sqrt{(\rho+\delta)^2h^2 - 4\,(A^2\eta/c)\,h^{2\eta}}}{2\,(A^2\eta/c)\,h^{2\eta}}, \end{aligned} \tag{B.3}$$

describing the two distinct segments of the $\dot{\theta} = 0$ nullcline with $\theta_1(h)$ and $\theta_2(h)$ being the upper and the lower segment, respectively. They meet above $\tilde{h}$ where $\theta_1(\tilde{h}) = \theta_2(\tilde{h}) > 0$, and their domain is the subset $\tilde{h} \leq h \leq \bar{h}$ of the real line.

By factoring out h in the numerator of the equation for $\theta_2(h)$, we have

$$\theta_2(h) = \frac{(\rho+\delta)h - h\sqrt{(\rho+\delta)^2 - 4\,(A^2\eta/c)\,h^{2\eta-2}}}{2\,(A^2\eta/c)\,h^{2\eta}},$$

from which it follows that $\lim_{h\to\infty} \theta_2(h) = 0$ with $\theta_2(h)$ asymptotically approaching zero from above, so $\theta_2(h) > 0$ over its domain. Differentiating $\theta_2(h)$ with respect to h yields an expression of the form

$$\frac{c\big(\sqrt{(\rho+\delta)^2h^2 - 4\,(A^2\eta/c)\,h^{2\eta}} - (\rho+\delta)h\big)}{A^2h^{2\eta+1}} + \frac{c\big((\rho+\delta) - \frac{2h(\rho+\delta)^2 - (8A^2\eta^2h^{2\eta-1})/c}{2\sqrt{(\rho+\delta)^2h^2 - 4\,(A^2\eta/c)\,h^{2\eta}}}\big)}{2A^2\eta h^{2\eta}},$$

the first part of which is negative, and the second part of which approaches $-\infty$ when $h \downarrow \tilde{h}$ as the radicand in the numerator tends to zero. This shows that over $\tilde{h}$ the slope of $\theta_2(h)$ is $-\infty$. It is also straightforward to demonstrate that $\theta_2(h)$ is strictly decreasing, and that $\lim_{h\to\infty} \theta_2'(h) = 0$.

Plausibly, these characteristics taken together suggest that $\theta_2(h)$ is strictly convex, but formally no general statement about convexity can be made. The characteristics of $\theta_2(h)$ over $\tilde{h}$ and at infinity exclude the possibility of strict concavity, so we only need to exclude weak convexity by showing that the curve has neither straight segments nor kinks. Both would mean that there is more than one h where the first differential of $\theta_2(h)$ has the same value, but this problem can only be resolved numerically for distinct parameter values. Weak convexity could also be excluded by showing that the second differential cannot be zero, but the most we can provide here are numerical solutions for h depending on the parameters that show the second differential does not vanish for any $h \geq \tilde{h}$. A third strategy could be built on the first-order Taylor polynomial underestimating $\theta_2(h)$ at any h if it was strictly convex; along this path, we cannot show uniqueness of any h where $\theta_2(h)$ and the Taylor polynomial have osculation.

Monotonicity of $\theta_1(h)$ crucially depends on η. It is obvious that for $0 < \eta < 0.5$ the function $\theta_1(h)$ in (B.3) is the sum of two strictly increasing terms, so it is strictly increasing. By simple algebra (B.3) can also be rewritten as

$$\theta_1(h) = \frac{(\rho+\delta) + \sqrt{(\rho+\delta)^2 - 4\,(A^2\eta/c)\,h^{2\eta-2}}}{2\,(A^2\eta/c)\,h^{2\eta-1}},$$

in which the numerator tends to $2(\rho+\delta)$ when $h \to \infty$ for any $0 < \eta < 1$. The term in the denominator, however, tends to infinity if $1 > \eta > 0.5$; hence $\theta_1(h) \to 0$ in this case. By contrast, if $0 < \eta < 0.5$, the asymptotic behavior of $\theta_1(h)$ is given by

$$\lim_{h\to\infty} \theta_1(h) = \frac{c(\rho+\delta)}{A^2\eta}\, h^{\,1-2\eta}. \tag{B.4}$$

Therefore, for $0 < \eta < 0.5$ the curve $\theta_1(h)$ is strictly increasing tending to infinity as $h \to \infty$, but it asymptotically approaches zero in cases where $0.5 < \eta < 1$. The first differential of $\theta_1(h)$ clearly shows that its slope over $\tilde{h}$ is $+\infty$, so in the $0.5 < \eta < 1$ case there must be a finite h where $\theta_1(h)$ attains a global maximum. By direct calculation this unique value of $h > 0$ is

$$\left(\frac{c(2\eta-1)^2(\rho+\delta)^2}{4A^2\eta^3}\left(\frac{2\eta}{2\eta-1}-1\right)\right)^{1/(2\eta-2)}.$$

The uniqueness of the steady state demonstrated in Proposition 1 ensures that even if all three curves tend to zero at infinitely high values of h, there is only one point of intersection, so the two sections of the $\dot{\theta} = 0$ nullcline keep the $\dot{h} = 0$ nullcline trapped in the $0.5 < \eta < 1$ case. It can also be shown that the point (h^*, θ^*) is always on $\theta_2(h)$.

Appendix C

Proposition 2: For $0 < \eta < 0.5$, the steady state characterized by the point (h^*, θ^*) in the $S = (h, \theta)$ space is saddle-path stable, so for any h_0 such that $1 < h_0 < h^*$ there exists a unique $\theta(0)$ from which the system defined by (3.4) and (3.5) converges to (h^*, θ^*) along a stable manifold with $\dot{h} > 0$ and $\dot{\theta} < 0$. The optimal path toward the steady state is unique.

Proof. First, we examine the sign of $\dot{h}$ above and below the $\dot{h} = 0$ nullcline. For any $0 < \eta < 0.5$ the $\dot{h} = 0$ nullcline takes all values of θ between 0 and $+\infty$, so the nullcline divides the positive quadrant of the $S = (h, \theta)$ space. Using this fact and the strict monotonicity of the nullcline, for any h there is a unique θ identifying the unique point in S where $\dot{h} = 0$ and from which one can leave the nullcline vertically. Therefore, at any h we may differentiate (A.1) with respect to θ, which yields

$$\frac{\partial \dot{h}}{\partial \theta} = \frac{A^2}{c}\, h^{2\eta} > 0,$$

implying that $\dot{h} > 0$ above the $\dot{h} = 0$ nullcline.

Second, we examine the sign of $\dot{\theta}$ to the left and to the right of the $\dot{\theta} = 0$ nullcline. By the same token as in the first part, at any θ we can find an h such that $\dot{\theta} = 0$. To see what happens to $\dot{\theta}$ when we leave the nullcline to the left, differentiate (A.3) with respect to h to obtain

$$\frac{\partial \dot{\theta}}{\partial h} = -\frac{A^2 \eta}{c}(2\eta - 1)\,\theta^2 h^{2\eta-2} + h^{-2} > 0$$

for any $0 < \eta < 0.5$. Hence, if we move horizontally left from the $\dot{\theta} = 0$ nullcline at a given θ by reducing h, then $\dot{\theta}$ decreases and $\dot{\theta} < 0$ emerges.

These sign properties of the vector field show that the steady state is saddle-path stable with well-defined directions of flow in the phase diagram. The dynamics of the system are effectively summarized in Fig. 14.

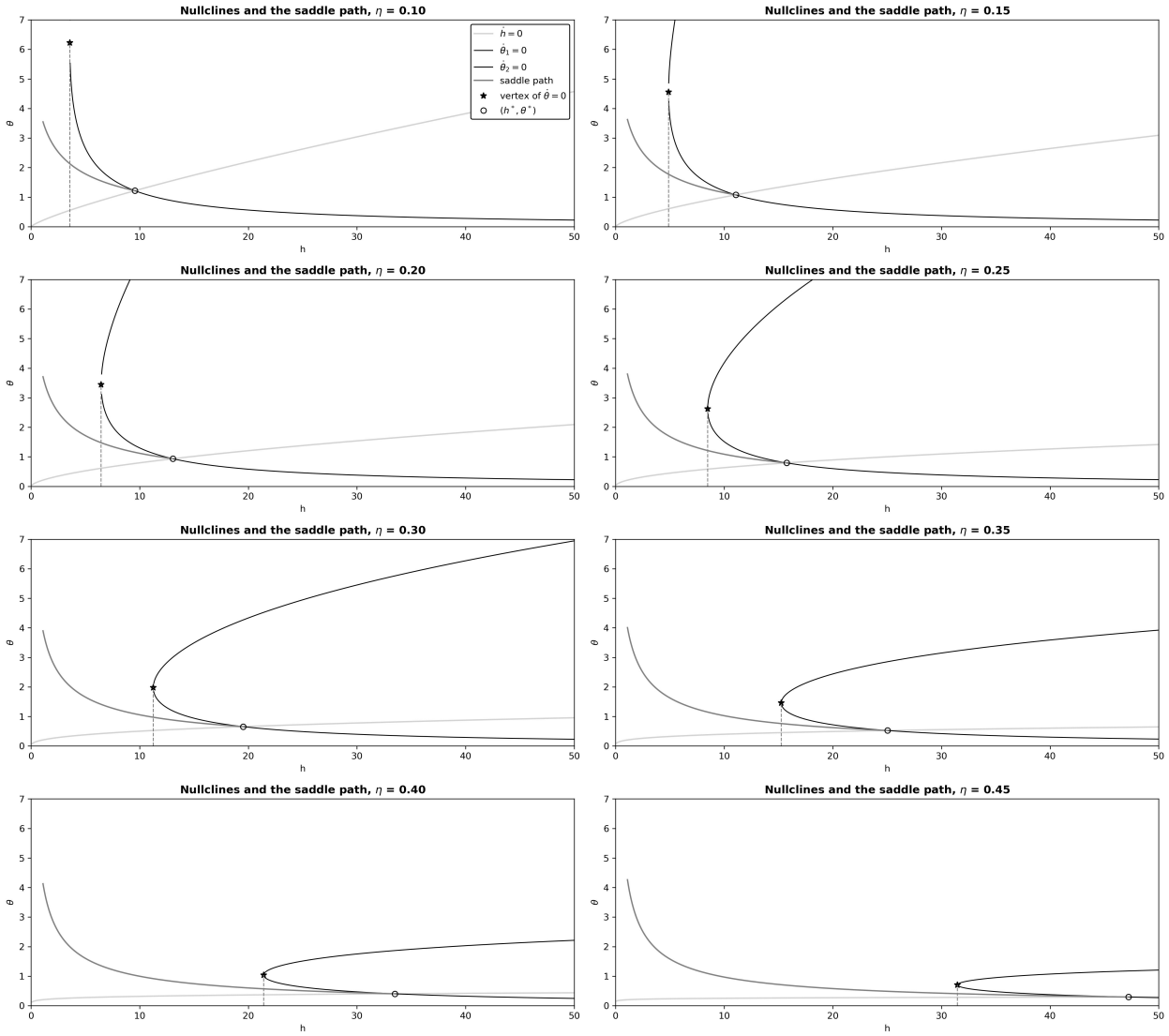


Figure 14: **Saddle-path stability in the model of school learning.**

From this analysis, $\dot{h} > 0$ and $\dot{\theta} < 0$ for any $h < h^*$ emerge as the key result, which is our starting point in the analysis of the optimum path of capital. For the other case, where $0.5 < \eta < 1$, we do not have clear results. It is easy to find a point along the $\dot{\theta} = 0$ nullcline where, after leaving the nullcline to the left, we find ourselves to the right of the same nullcline (see point A in Fig. 2, Pane B above); or, likewise, a point where, after leaving the nullcline upwards, we find ourselves below the same nullcline (point B). We thus disregard the $0.5 < \eta < 1$ case.

The linearization of the implied dynamics reassures saddle-path stability in the $0 < \eta < 0.5$ case. The parameter matrix of the linearized system around the steady state is the Jacobian

$$J = \begin{bmatrix} J_{11} & J_{12} \\ J_{21} & J_{22} \end{bmatrix} = \begin{bmatrix} \frac{\partial \dot{h}}{\partial h} & \frac{\partial \dot{h}}{\partial \theta} \\ \frac{\partial \dot{\theta}}{\partial h} & \frac{\partial \dot{\theta}}{\partial \theta} \end{bmatrix} = \\ \begin{bmatrix} \frac{2\eta A^2}{c}\,\theta^*(h^*)^{2\eta-1} - \delta & \frac{A^2}{c}(h^*)^{2\eta} \\ (1-2\eta)\frac{\eta A^2}{c}(\theta^*)^2(h^*)^{2\eta-2} + (h^*)^{-2} & (\rho+\delta) - \frac{2\eta A^2}{c}\,\theta^*(h^*)^{2\eta-1} \end{bmatrix}.$$

Here $\partial\dot{h}/\partial h$, $\partial\dot{h}/\partial\theta$, etc. denote the first-order differentials of (3.10) and (3.11) which are evaluated at the steady state. Obviously $J_{12} > 0$, and $J_{21} > 0$ also holds for $0 < \eta < 0.5$. Substituting h^* and θ^* into J_{11} and J_{22}, by direct calculation we obtain

$$J_{11} = \delta(2\eta - 1) < 0, \qquad J_{22} = \rho + \delta(1 - 2\eta) > 0,$$

for the relevant case $0 < \eta < 0.5$. Thus the general form of the Jacobian is

$$J = \begin{bmatrix} - & + \\ + & + \end{bmatrix},$$

from which it follows that the determinant of J is negative. Using the basic fact that the determinant of J equals the product of its eigenvalues, it follows that one eigenvalue is strictly positive while the other is strictly negative. Moreover, the negative determinant also implies that both eigenvalues are real (Horn & Johnson, 2013, pp. 50–51). Consequently, with two real eigenvalues of opposite signs, the system is saddle-path stable in a sufficiently large neighborhood of the steady state.

It is also straightforward to prove that the elements of the eigenvector associated with the stable eigenvalue $\lambda_s < 0$ have mixed signs. The eigenvector $[v_1\ v_2]^T$ solves

$$\begin{bmatrix} \lambda_s & 0 \\ 0 & \lambda_s \end{bmatrix} \begin{bmatrix} v_1 \\ v_2 \end{bmatrix} = \begin{bmatrix} J_{11} & J_{12} \\ J_{21} & J_{22} \end{bmatrix} \begin{bmatrix} v_1 \\ v_2 \end{bmatrix},$$

implying two linear equations. We want to prove that v_1 and v_2 have opposite signs. Assume the contrary, i.e. $v_i > 0$ or $v_i < 0$, $i = 1, 2$. In the second equation, if $v_i > 0$, then $J_{21}v_1 + J_{22}v_2 > 0$, while $\lambda_s v_2 < 0$, a contradiction. In the opposite case, if $v_i < 0$, then $J_{21}v_1 + J_{22}v_2 < 0$, while $\lambda_s v_2 > 0$, again a contradiction. Thus v_1 and v_2 must have opposite signs.

It follows that when the state initially deviates from its steady-state value in the negative direction along the stable manifold, i.e. $\tilde{h}(0) = h_0 - h^* < 0$, then the costate deviates in the positive direction, i.e. $\tilde{\theta}(0) = \theta(0) - \theta^* > 0$. Formally, given that $\tilde{h}(t) = \tilde{h}(0)e^{\lambda_s t}$, we have

$$\dot{\tilde{h}}(t) = \tilde{h}(0)\lambda_s e^{\lambda_s t} > 0, \qquad \dot{\tilde{\theta}}(t) = \frac{v_2}{v_1}\tilde{h}(0)\lambda_s e^{\lambda_s t} < 0,$$

since $\tilde{h}(0) < 0$, $\lambda_s < 0$, and $v_2/v_1 < 0$, and $\tilde{\theta}(t) = v_2/v_1\, \tilde{h}(t) = v_2/v_1\, \tilde{h}(0)\, e^{\lambda_s\, t}$. Therefore, along the stable manifold, $\dot{h}(t) > 0$ starting from $h_0 < h^*$ and $\dot{\theta}(t) < 0$.

As a final step in the proof, when $0 < \eta < 0.5$, the optimized Hamiltonian is strictly concave in h, so the optimal path is unique. To see this, let $\hat{u}$ denote the control path that maximizes the Hamiltonian in (3.8). Then the maximized Hamiltonian is

$$H^0(h;\theta;u) \equiv H(h;\theta;\hat{u}) = \ln h - \frac{c}{2}\hat{u}^{\,2} + \theta(Ah^{\eta}\hat{u} - \delta h),$$

the second differential of which with respect to h is

$$-h^{-2} + \eta(\eta-1)A\theta h^{\eta-2}\hat{u} < 0,$$

implying the strict concavity of H^0. The optimal path toward the steady state is therefore unique.

□

Appendix D

By using (3.9) and (3.11), the second differential of h is

$$\ddot{h} = \frac{A^2}{c}\left(\dot{\theta}\, h^{2\eta} + 2\eta\theta h^{2\eta-1}\dot{h}\right) - \delta\dot{h}, \tag{D.1}$$

which might be positive; hence the optimum path of h might be strictly concave or might have convex sections as $\dot{\theta} < 0$ and $\dot{h} > 0$ all along the path with $\lim_{t\to\infty}\dot{h}(t) = 0$ and $\lim_{t\to\infty}\dot{\theta}(t) = 0$. Substituting from (3.10) and (3.11) we can trace (D.1) back to the dynamics of h and θ, and obtain an expression that can be used as a criterion for convexity, given as

$$\frac{A^2\eta}{c}\left(\theta h^{2\eta-1}\right)^2 + (\rho - 2\eta\delta)\,\theta h^{2\eta-1} + \frac{c\delta^2}{A^2} > h^{2\eta-2}, \tag{D.2}$$

in which the inequality holds for convex sections of the path of h; the opposite inequality characterizes concave sections. Note that the left-hand side of (D.2) is a quadratic polynomial in the variable $\theta h^{2\eta-1}$, the roots of which are

$$\frac{-(\rho - 2\eta\delta) \pm \sqrt{(\rho-2\eta\delta)^2 - 4\,(A^2\eta/c)\,(c\delta^2/A^2)}}{(2A^2\eta)/c}.$$

Since $\rho - 2\eta\delta$ is likely to be positive for sufficiently low values of δ, the polynomial has no positive roots in typical parameter configurations. A strictly concave path of h is summarized in Fig. 15 below.

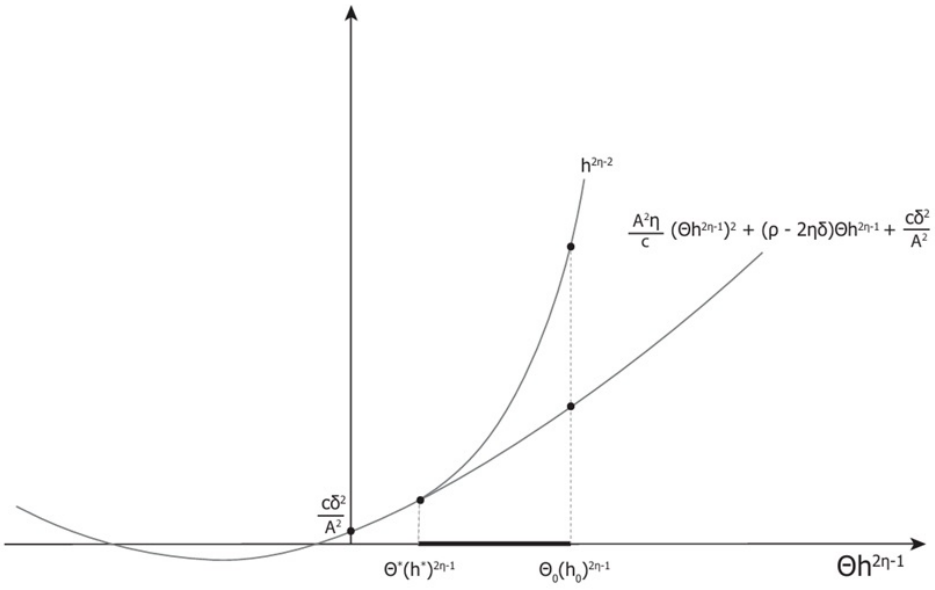


Figure 15: **If the optimum path of h is strictly concave, then the second-order polynomial in $\theta h^{2\eta-1}$ remains under the curve $h^{2\eta-2}$.**

As $\dot{\theta} < 0$ and $\dot{h} > 0$, and $0 < \eta < 0.5$, the ratio $\theta h^{2\eta-1}$ (or, equivalently, $\theta/h^{1-2\eta}$) attains its highest value at h_0 and θ_0, and the learning process reduces it to $\theta^*/(h^*)^{1-2\eta}$, which, by using (A.7), equals $\delta c/A^2$ in all possible cases. Therefore, the lower bound of the state space defined in $\theta/h^{1-2\eta}$ is fixed at this point. Moreover, any point of an optimum path can be represented as a unique point in $\theta/h^{1-2\eta}$ since, by the strict monotonicity of the dynamics of the state and the costate, any pair (h, θ) takes a unique value in $\theta/h^{1-2\eta}$. From this it follows that along any optimum path the position of $h^{2\eta-2}$ in Fig. 15 is clearly defined because to any value of the form $\theta/h^{1-2\eta}$ there corresponds a unique h; hence for strict concavity $h^{2\eta-2}$ serves as an upper bound for the left-hand side of (D.2).

By direct calculation, (D.2) holds with equality at $\theta^*/(h^*)^{1-2\eta}$ (i.e., at the lower bound), so there $\ddot{h} = 0$; at the end of the optimum path the trajectory is neither concave nor convex. It is also straightforward to note that $\dot{h} = 0$ at h^*, and these two features together with $\dot{h} > 0$ below the optimum capital stock imply that strict convexity of $h(t)$ can be excluded. Right before reaching h^* the very latest a flat section of $h(t)$ inevitably emerges. If convex sections exist, they occur in the earlier phases of human capital accumulation. They may appear because, by differentiating (3.11) with respect to time at $u = 1$, one can obtain a strictly convex section reaching up to relatively high values of h. The easiest way to find a convex section is to raise the starting value of the left-hand side expression in (D.2) above $h^{2\eta-2}$, if possible. Doing so could produce an optimum path that starts with a convex section which fades away; as noted, the left-hand side expression approaches $h^{2\eta-2}$ from below near the optimum. Multiple convex sections cannot be excluded. The most we can say about a partly convex case is the possible existence of an initial convex phase and a final flat section along the optimum path.

By changing the starting values h_0 and $\theta(0)$ we may therefore find an upper bound for the state space in $\theta/h^{1-2\eta}$ in Fig. 15 that implies (D.2) with the inequality signaling convexity. Two details must be noted. First, since $\dot{\theta} < 0$, a lower $h_0 > 1$ implies a higher $\theta(0) > 0$ ceteris paribus as a starting value along a stable manifold. Second, even if two students start from the same h_0, a higher η implies a higher h^*; the larger the gap between h_0 and the optimum knowledge level, the scarcer and hence more valuable the same h_0 becomes, leading to a higher $\theta(0)$.

Appendix E

Proposition 3: The constrained form of the problem defined by (3.4) and (3.5) where $u(t) = 1$ has a unique steady state h_c^* and θ_c^*. These solutions are finite for any configuration of appropriate and finite parameters.

Proof. In Section 3 we showed that there is a unique and finite maximum maintainable capital stock $\bar{h}$ obtained by setting $u(t) = 1$ and $\dot{h} = 0$ in (3.11). Hence we set $h_c^* \equiv \bar{h}$, which is the $\dot{h}_c = 0$ nullcline of the constrained process. Applying $u(t) = 1$ to (3.10), the dynamics of the costate are described by

$$\dot{\theta}_c = \theta(\rho + \delta - A\eta h_c^{\eta-1}) - \frac{1}{h_c}. \tag{E.1}$$

A steady state must lie on both the $\dot{h}_c = 0$ and $\dot{\theta}_c = 0$ nullclines, so $h_c = h_c^*$, $\theta_c = \theta_c^*$, and $\dot{\theta}_c = 0$ in (E.1). Solving $\dot{\theta}_c = 0$ for the steady state yields

$$\theta_c^* = \frac{(\delta/A)^{1/(1-\eta)}}{\rho + \delta(1-\eta)} = \frac{h_c^*}{\rho + \delta(1-\eta)},$$

which is unique and finite provided h_c^* is finite and $\rho + \delta(1-\eta) > 0$. □

Now that the system in (3.10) and (3.11) converges toward a unique steady state under the constraint $u(t) = 1$, we check stability by linearizing the constrained dynamics

$$\dot{h}_c = Ah_c^{\eta} - \delta h_c \tag{E.2}$$

and (E.1) around the steady state.

Proposition 4: The steady state h_c^* and θ_c^* of the constrained process is stable.

Proof. Differentiating (E.1) and (E.2) with respect to h and θ, the constrained process has the Jacobian

$$J^c = \begin{bmatrix} J_{11}^c & J_{12}^c \\ J_{21}^c & J_{22}^c \end{bmatrix} = \begin{bmatrix} \frac{\partial \dot{h}_c}{\partial h} & \frac{\partial \dot{h}_c}{\partial \theta} \\ \frac{\partial \dot{\theta}_c}{\partial h} & \frac{\partial \dot{\theta}_c}{\partial \theta} \end{bmatrix}.$$

Evaluating the partial derivatives at the steady state gives

$$J^c = \begin{bmatrix} \delta(\eta - 1) & 0 \\ A\eta(1-\eta)\,(A/\delta)^{(\eta-3)/(1-\eta)}/(\rho + \delta(1-\eta)) + (A/\delta)^{-2/(1-\eta)} & \rho + \delta(1-\eta) \end{bmatrix},$$

so that $J^c_{11} < 0$, $J^c_{12} = 0$, $J^c_{21} > 0$, and $J^c_{22} > 0$. The determinant of J^c is negative, hence the Jacobian has two real nonzero eigenvalues of opposite signs and the constrained process is saddle-path stable. Therefore, for any starting value $1 < h_c(0) < h^*_c$ there exists a unique $\theta_c(0)$ from which the paths $h_c(t)$ and $\theta_c(t)$ converge to h^*_c and θ^*_c, respectively. The dynamics of $\dot{h}_c$ in (E.2) does not depend on $\theta_c(t)$, while $h_c(t)$ enters the equation of $\dot{\theta}_c$ in (E.1), and accordingly under any appropriate parameter configuration specified earlier there is a unique path for $\theta_c(t)$ along which the constrained process reaches its steady state.

Let $\lambda^c_s < 0$ denote the stable eigenvalue and $[v^c_1 \; v^c_2]^T$ the associated eigenvector solving

$$\begin{bmatrix} \lambda^c_s & 0 \\ 0 & \lambda^c_s \end{bmatrix} \begin{bmatrix} v^c_1 \\ v^c_2 \end{bmatrix} = \begin{bmatrix} J^c_{11} & J^c_{12} \\ J^c_{21} & J^c_{22} \end{bmatrix} \begin{bmatrix} v^c_1 \\ v^c_2 \end{bmatrix}.$$

By the same contradiction argument as in Proposition 2, v^c_1 and v^c_2 must have opposite signs. Hence along the stable manifold $\dot{h}_c(t) > 0$ and $\dot{\theta}_c(t) < 0$. □

In the simplest case, $\dot{u}(t) < 0$ in the unconstrained process with possibly $u(t) > 1$ for a period $t \in [0, T)$ and $u(T) = 1$; T is the time when the exterior path of $u(t)$ becomes interior. Due to saddle-path stability of the unconstrained problem, there is a unique pair $h(T)$ and $\theta(T)$ associated with this switching time. In such a case we can split the original problem. For the initial period with the exterior solution we use the constrained problem to describe the dynamics of human capital with $\dot{h}_c(t) > 0$ starting from the unconstrained initial value $h_c(0) = h_0$. Once the constrained dynamics reaches $h(T)$, the unconstrained part of the problem begins with $u(t) \leq 1$ until h^* and θ^* are reached. Thus $h(T)$ of the original problem with an exterior solution becomes the boundary condition for the unconstrained phase. We switch from the constrained to the unconstrained problem with a jump in the costate at T. This pattern generalizes to more complex switching sequences.

Appendix F

Proposition 5: There exists a unique maximum level of knowledge $\bar{h}_i$, $i = 1, 2$, for each agent, above which no capital stock is maintainable under the constraint $0 \leq u_i(t) \leq 1$.

Proof. These upper bounds are obtained where $\dot{h}_1 = \dot{h}_2 = 0$ and $u_1 = u_2 = 1$. Hence we have the two-equation system for the maximum levels:

$$A\bar{h}_2^{\gamma/2}\,\bar{h}_1^{\eta_1+\gamma/2} = \delta\bar{h}_1, \tag{F.1a}$$

$$A\bar{h}_1^{\gamma/2}\,\bar{h}_2^{\eta_2+\gamma/2} = \delta\bar{h}_2. \tag{F.1b}$$

These equations are to be solved for $\bar{h}_1$ and $\bar{h}_2$. From (F.1a) it follows that

$$\bar{h}_1 = \left(\frac{A}{\delta}\right)^{\frac{1}{1-\eta_1-\frac{\gamma}{2}}} \bar{h}_2^{\frac{\gamma}{2(1-\eta_1-\frac{\gamma}{2})}}, \tag{F.2}$$

so $\bar{h}_1 = f(\bar{h}_2)$, where

$$0 < \frac{\gamma}{2(1-\eta_1-\frac{\gamma}{2})} < 1$$

.

Thus $\bar{h}_1$ is an increasing function of the (potentially infinite) $\bar{h}_2$; note that we do not a priori assume finiteness of any $\bar{h}_i$.

By symmetry, from (F.1b) we obtain

$$\bar{h}_2 = \left(\frac{A}{\delta}\right)^{\frac{1}{1-\eta_2-\frac{\gamma}{2}}} \bar{h}_2^{\frac{\gamma}{2(1-\eta_2-\frac{\gamma}{2})}}, \tag{F.3}$$

so $\bar{h}_2 = g(\bar{h}_1)$. Combining (F.2) and (F.3) yields the fixed-point relation $\bar{h}_1 = f(g(\bar{h}_1))$. Explicitly,

$$\bar{h}_1 = \left(\frac{A}{\delta}\right)^{\frac{1-\eta_2}{(1-\eta_1-\frac{\gamma}{2})(1-\eta_2-\frac{\gamma}{2})}} \bar{h}_1^{\frac{\gamma^2}{4(1-\eta_1-\frac{\gamma}{2})(1-\eta_2-\frac{\gamma}{2})}}.$$

Solving this fixed-point equation gives

$$\bar{h}_1 = \left(\frac{A}{\delta}\right)^{\frac{4-4\eta_2}{4(1-\eta_1-\frac{\gamma}{2})(1-\eta_2-\frac{\gamma}{2})-\gamma^2}}$$

and by symmetry

$$\bar{h}_2 = \left(\frac{A}{\delta}\right)^{\frac{4-4\eta_1}{4(1-\eta_1-\frac{\gamma}{2})(1-\eta_2-\frac{\gamma}{2})-\gamma^2}}$$

Both $\bar{h}_1$ and $\bar{h}_2$ are finite and unique under the parameter configurations that make the exponents well defined, so we can expect finite solutions for the equilibrium knowledge levels. □

Appendix G

Proposition 6: Regarding the equilibrium capital stock h_1^e, the differential $\partial h_1^e/\partial \eta_2 > 0$ holds as long as the condition

$$\frac{(A^2/(\delta c))}{\rho + \delta(1-\eta_i-\gamma/2)} > 1 \tag{G.1}$$

is satisfied for $i = 1, 2$.

Proof. Note that η_2 appears in three places in (6.8). Instead of calculating $\partial h_1^e/\partial \eta_2$ directly, we first compute the differentials of these constituent parts. Accordingly, we obtain

$$\frac{d}{d\eta_2}\left(\frac{(A^2/(\delta c))}{\rho + \delta(1-\eta_2-\gamma/2)}\right) = \frac{A^2/c}{\big(\rho + \delta(1-\eta_2-\gamma/2)\big)^2} > 0, \tag{G.2}$$

$$\frac{d}{d\eta_2}\left(\frac{2-2\eta_2-\gamma}{(2\eta_1+\gamma-2)(2\eta_2+\gamma-2)-\gamma^2}\right) = \frac{\gamma^2}{2\big(\gamma\eta_1 - 2\gamma - 2\eta_1 + \eta_2(2\eta_1+\gamma-2)+2\big)^2} > 0, \tag{G.3}$$

and

$$\frac{d}{d\eta_2}\left(\frac{\gamma}{(2\eta_1+\gamma-2)(2\eta_2+\gamma-2)-\gamma^2}\right)=\frac{\gamma(4-4\eta_1-2\gamma)}{\left((2\eta_1+\gamma-2)(2\eta_2+\gamma-2)-\gamma^2\right)^2}>0, \quad \text{(G.4)}$$

where the inequality in (G.4) follows from the requirement $\eta_i+\gamma/2<0.5$, which implies $2>4\eta_1+2\gamma$. The same requirement ensures that the denominators in (G.3) and (G.4) are strictly positive.

Thus all three components—the second base and both exponents—are increasing functions of η_2. By the monotonicity properties of power functions, h_1^e is an increasing function of η_2 provided the bases in (6.8) exceed 1, which is ensured by condition (G.1). □

Note that we expect (G.1) to hold following from (A.7) and the initial condition $h_i(0)>1$. Consequently $\partial h_1^e/\partial\eta_2>0$: the equilibrium knowledge level of the family with superior learning ability increases with the learning ability of the other family. Intuitively, this aligns with the idea that a classmate with inferior learning potential holds back her peer in an environment where learning abilities interact through an external effect.

By similar arguments we obtain $\partial h_1^e/\partial\eta_1>0$.

Proposition 7: Regarding the equilibrium capital stock h_1^e, the differential $\partial h_1^e/\partial\eta_1>0$ holds under the same condition (G.1) for $i=1,2$.

Proof. Due to the symmetry of (6.8) in η_1 and η_2, the analogues of (G.2) with η_1 replacing η_2 and of (G.4) apply directly. For the remaining term we have

$$\frac{d}{d\eta_1}\left(\frac{2-2\eta_2-\gamma}{(2\eta_1+\gamma-2)(2\eta_2+\gamma-2)-\gamma^2}\right)=\frac{2(2\eta_2+\gamma-2)^2}{\left((2\eta_1+\gamma-2)(2\eta_2+\gamma-2)-\gamma^2\right)^2}>0,$$

where the denominator is strictly positive for the same reason used in the case of (G.4). As long as (G.1) holds, the monotonicity of the power function implies $\partial h_1^e/\partial\eta_1>0$. □

By symmetry of the two equations in (6.8), we also have $\partial h_2^e/\partial\eta_1>0$ (analogue of Proposition 6) and $\partial h_2^e/\partial\eta_2>0$ (analogue of Proposition 7). The assumption $\eta_1>\eta_2$ does not affect the generality of these results. Since $\partial h_1^e/\partial\eta_2>0$ and $\partial h_2^e/\partial\eta_1>0$ while $\eta_1>\eta_2$, we can interchange η_1 and η_2 in (6.8) to obtain the corresponding relations for the other agent. Consequently, the equilibrium stock of each agent i is positively related to η_j of agent j, for $i\neq j$.

Appendix H

Proposition 8: The equilibrium allocation with $h_1^e,\ h_2^e,\ \theta_1^e$ and θ_2^e is stable.

Proof. For a formal proof, it suffices to return to the linearized dynamics of the isolated individual as carried out in Appendix C. In the equilibrium setting we obtain an analogous Jacobian with which we check whether, when perturbed away from the equilibrium, an individual's capital stock returns to the equilibrium state.

Given (6.5), the entry J_{11} for Agent 1 becomes, after substitution of h_2^e and θ_1^e,

$$J_{11} =$$

$$\frac{2(\eta_1+\gamma/2)A^2(h_2^e)^\gamma}{c}\ \frac{\delta c}{A^2(h_2^e)^\gamma}\left[\frac{(A^2(h_2^e)^\gamma)/(\delta c)}{\rho+\delta(1-\eta_1-\gamma/2)}\right]^{\frac{1-2(\eta_1+\gamma/2)}{2-2(\eta_1+\gamma/2)}}\left[\frac{(A^2(h_2^e)^\gamma)/(\delta c)}{\rho+\delta(1-\eta_1-\gamma/2)}\right]^{\frac{2(\eta_1+\gamma/2)-1}{2-2(\eta_1+\gamma/2)}}$$

$$-\delta,$$

which simplifies to

$$J_{11} = 2(\eta_1+\gamma/2)\delta-\delta = \delta\big[2(\eta_1+\gamma/2)-1\big] < 0,$$

under the assumption $0 < \eta_1+\gamma/2 < 0.5$. By symmetry, for Agent 2 we obtain

$$J_{11} = \delta\big[2(\eta_2+\gamma/2)-1\big] < 0.$$

Similarly, the diagonal entry J_{22} for Agent 1 becomes

$$\begin{aligned} J_{22} &= (\rho+\delta) - \frac{2(\eta_1+\gamma/2)A^2(h_2^e)^\gamma}{c}\,\theta_1^*(h_2^e)^{2\eta-1} \\ &= (\rho+\delta) - 2\delta(\eta_1+\gamma/2) = \rho+\delta\big[1-2(\eta_1+\gamma/2)\big] > 0, \end{aligned}$$

again under $0 < \eta_1+\gamma/2 < 0.5$. By symmetry, for Agent 2 we have

$$J_{22} = \rho+\delta\big[1-2(\eta_2+\gamma/2)\big] > 0.$$

It is straightforward to verify that the off-diagonal social equilibrium analogues J_{12} and J_{21} are both positive. Hence the Jacobian of the social equilibrium has the sign pattern

$$J = \begin{bmatrix} - & + \\ + & + \end{bmatrix},$$

so its determinant is negative. A negative determinant implies that the two eigenvalues are real and have opposite signs; therefore the equilibrium is saddle-path stable for both agents.

Thus, small deviations from the equilibrium induce dynamics that return the system along the stable manifold, and the equilibrium allocation $(h_1^e, h_2^e, \theta_1^e, \theta_2^e)$ is stable. □

Appendix I

Proposition 9: Function $h(h_1^*)$ in (6.20) uniquely determines the optimal capital stock $h_1^* > 0$.

Proof. It suffices to show that $h(h_1^*)$ is strictly increasing in h_1^*. If so, there is a unique h_1^* where the curve $h(h_1^*)$ crosses the horizontal line on the left.

The positivity of the multiplier in the braces in (6.20) is straightforward to prove by assuming positivity and showing that no contradiction follows. This assumption directly implies

$$\frac{2[\delta\rho c+\delta^2 c(1-\eta_1-\gamma/2)]}{\delta^2\gamma c} > \frac{2[\delta\rho c+\delta^2 c(1-\eta_1-\gamma/2)]+\delta^2\gamma c}{2[\delta\rho c+\delta^2 c(1-\eta_2-\gamma/2)]+\delta^2\gamma c}.$$

After expansion and simplification, the terms in the inequality are of the types $c^2\delta^2$, $c^2\delta^3$ and $c^2\delta^4$. By grouping the expressions, it follows that the multiplier in (6.20) is positive if

$$2c^2\delta^4\big[2(1-\eta_1-\eta_2-\gamma)+\gamma(\eta_1+\eta_2)+2\eta_1\eta_2\big] > 0 \tag{G.1}$$

and

$$4\delta^3\rho c^2(2-\eta_1-\eta_2-\gamma) > 0. \tag{G.2}$$

The second inequality (G.2) obviously holds under the parameter restrictions, and the first (G.1) holds under the previous assumption that $0 < \eta_j + \gamma/2 < 0.5$, which implies $1-\eta_1-\eta_2-\gamma > 0$.

To ensure that $h(h_1^*)$ is strictly increasing we also need the exponent in (6.20) to be positive. This requires

$$(2-\gamma)(1-\eta_1-\eta_2)-\gamma+2\eta_1\eta_2 > 0, \tag{G.3}$$

which by simple algebra reduces to the condition

$$1-\eta_1-\eta_2-\gamma > 0.$$

Under these parameter restrictions the multiplier in (6.20) is positive and the exponent is positive, so $h(h_1^*)$ is strictly increasing in h_1^*. Therefore there exists a unique $h_1^* > 0$ solving the optimality condition. □

Appendix J

Proposition 10: The unique optimum capital stock h_1^* as determined by $h(h_1^*)$ in (6.20) is an increasing function of η_2; therefore $\partial h_1^*/\partial\eta_2 > 0$.

Proof 1. We use equation (6.17c) to find the differential of h_1^* with respect to η_2. In the steady state $\dot\theta_1^* = 0$, therefore (6.17c) becomes

$$(\rho+\delta)\dot\theta_1^* = \frac{1}{h_1^*} + A(\eta_1+\gamma/2)\,\theta_1^*(h_1^*)^{\eta_1+\gamma/2-1}(h_2^*)^{\gamma/2}u_1^* + A\frac{\gamma}{2}\,\theta_2^*(h_1^*)^{\gamma/2-1}(h_2^*)^{\eta_2+\gamma/2}u_2^*.$$

Assuming that h_1^* depends on η_2, and proceeding by the envelope theorem and implicit differentiation (disregarding indirect effects of a change in η_2 on other variables), we obtain

$$-(h_1^*)^{-2}\,\frac{\partial h_1^*}{\partial\eta_2} - A(1-\eta_1-\gamma/2)(\eta_1+\gamma/2)\,\theta_1^*u_1^*(h_1^*)^{\eta_1+\gamma/2-2}(h_2^*)^{\gamma/2}\,\frac{\partial h_1^*}{\partial\eta_2}$$

$$-A(1-\gamma/2)\frac{\gamma}{2}\,\theta_2^* u_2^* (h_1^*)^{\gamma/2-2}(h_2^*)^{\eta_2+\gamma}\,\frac{\partial h_1^*}{\partial \eta_2} + A\frac{\gamma}{2}\,\theta_2^* u_2^* (h_1^*)^{\gamma/2-1}(h_2^*)^{\eta_2+\gamma/2}\ln(h_2^*) = 0.$$

This is a linear equation in $\partial h_1^*/\partial \eta_2$ with three coefficients multiplying $\partial h_1^*/\partial \eta_2$ and a remaining positive term. Under the stated assumptions $\gamma > 0$, $0.5 > \eta_i + \gamma/2 > 0$, and given $h_i^* > 0$, $\theta_i^* > 0$, $u_i^* > 0$ for $i = 1, 2$, the three coefficients on $\partial h_1^*/\partial \eta_2$ are negative while the fourth term is positive. Rearranging yields $\partial h_1^*/\partial \eta_2 > 0$. □

Proof 2. In (6.20) h_1^* is given by a power function. A sufficient condition for h_1^* to increase with η_2 (under the positivity condition $(2-\gamma)(1-\eta_1-\eta_2)-\gamma+2\eta_1\eta_2 > 0$ from Proposition 9) is that both the exponent of h_1^* and the multiplicative factor (multiplier) are decreasing functions of η_2. In that case the right-hand side curve flattens and crosses the left horizontal line at a higher h_1^*. This argument applies when $h_1^* > 1$, which can be ensured by appropriate parameter choices and the initial condition $h_1(0) > 1$.

The exponent of h_1^* in (6.20) is easily shown by direct differentiation to be a decreasing function of η_2. To show that the multiplier is decreasing in η_2, rewrite the multiplier in the form

$$\frac{\left(\dfrac{\delta\rho c+\delta^2 c(1-\eta_1-\gamma/2)}{A^2} - \dfrac{\delta^2\gamma c}{2A^2}\cdot\dfrac{2[\delta\rho c+\delta^2 c(1-\eta_1-\gamma/2)]+\delta^2\gamma c}{2[\delta\rho c+\delta^2 c(1-\eta_2-\gamma/2)]+\delta^2\gamma c}\right)}{\left(\dfrac{2[\delta\rho c+\delta^2 c(1-\eta_1-\gamma/2)]+\delta^2\gamma c}{2[\delta\rho c+\delta^2 c(1-\eta_2-\gamma/2)]+\delta^2\gamma c}\right)^{\gamma/(2-2\eta_2)}}, \tag{J.1}$$

in which the numerator is clearly decreasing in η_2. To obtain the desired result it suffices to show that the denominator is increasing in η_2. Differentiating the denominator with respect to η_2 and assuming that the differential is positive to prove by contradiction leads to the inequality

$$\ln\left[\frac{2\rho+2\delta(1-\eta_1-\gamma/2)+\delta\gamma}{2\rho+2\delta(1-\eta_2-\gamma/2)+\delta\gamma}\right] > -\frac{2\delta(1-\eta_2)}{2\rho+2\delta(1-\eta_2-\gamma/2)+\delta\gamma}. \tag{J.2}$$

The right-hand side of (J.2) is strictly increasing in η_2, and

$$\sup_{\eta_2\in(0,0.5)}\left[-\frac{2\delta(1-\eta_2)}{2\rho+2\delta(1-\eta_2-\gamma/2)+\delta\gamma}\right] = -\frac{\delta}{2\rho+\delta} < 0,$$

attained at $\eta_2 = 0.5$. The left-hand side is strictly increasing in η_2 as

$$\inf_{\eta_2\in(0,0.5)}\ln\left[\frac{2\rho+2\delta(1-\eta_1-\gamma/2)+\delta\gamma}{2\rho+2\delta(1-\eta_2-\gamma/2)+\delta\gamma}\right] = \ln\left[\frac{2\rho+2\delta(1-\eta_1-\gamma/2)+\delta\gamma}{2\rho+2\delta(1-\gamma/2)+\delta\gamma}\right],$$

is attained at $\eta_2 = 0$. Taking the infimum also over $\eta_1 \in (0, 0.5)$ yields

$$\inf_{\eta_1\in(0,0.5)}\inf_{\eta_2\in(0,0.5)}\ln\left[\frac{2\rho+2\delta(1-\eta_1-\gamma/2)+\delta\gamma}{2\rho+2\delta(1-\eta_2-\gamma/2)+\delta\gamma}\right] = \ln\left(\frac{\rho+\delta/2}{\rho+\delta}\right) < 0,$$

attained at $\eta_1 = 0.5$. Therefore, if

$$g(\delta,\rho) \equiv \ln\left(\frac{\rho+\delta/2}{\rho+\delta}\right) + \frac{\delta}{2\rho+\delta} > 0, \tag{J.3}$$

then $\dfrac{\partial h_1^*}{\partial \eta_2} > 0$ certainly holds. Note that $g(\delta,\rho)$ is not defined at $(\delta,\rho)=(0,0)$. On the δ-axis ($\rho=0$), $g(\delta,0)=\ln(1/2)+1>0$. On the ρ-axis ($\delta=0$), $g(0,\rho)=\ln(1)+0=0$. □

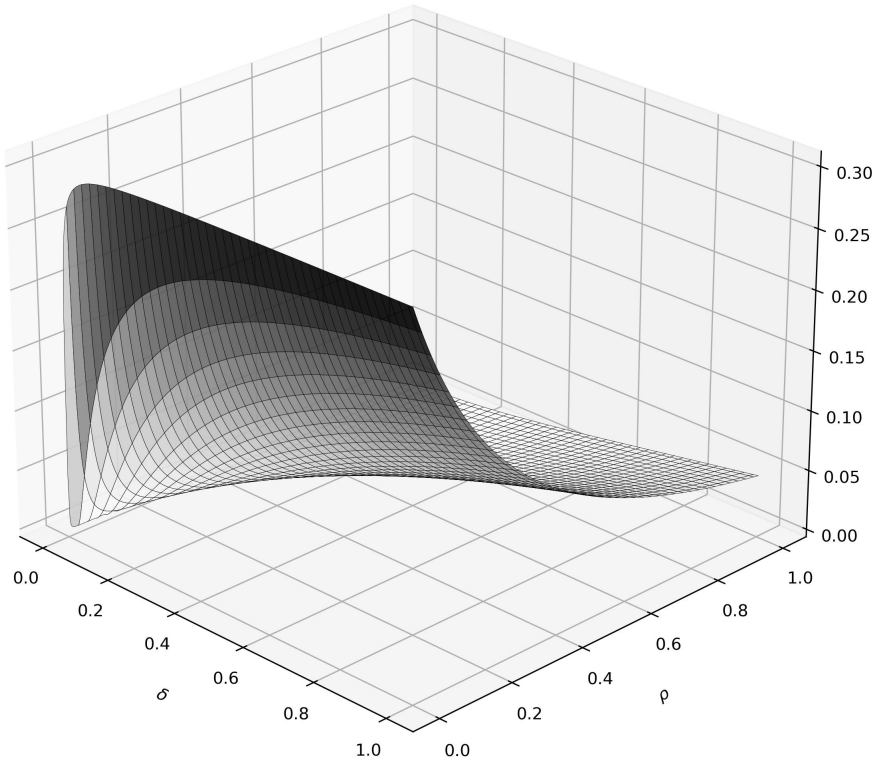


Figure 16: **The function $g(\delta,\rho)$ over the intervals $0<\delta<1$ and $0<\rho<1$.**

These cases, however, are irrelevant as some of the basic assumptions of the model are omitted (there is no discounting, or there is no capital depreciation). To see that $g(\delta,\rho)$ is strictly positive over the relevant domain $\delta>0$ and $\rho>0$, suffice it to evaluate its differential

$$\frac{\partial g}{\partial \delta} = \frac{\delta\rho}{(\delta+\rho)(\delta+2\rho)^2},$$

which is positive, so g is strictly increasing in δ for any $\rho>0$. Over the relevant domain, $\partial h_1^*/\partial\eta_2 > 0$ therefore holds. □

Proposition 11: The unique optimum capital stock h_2^* as determined by $h(h_1^*)$ in (6.20) and the term in (6.19) is increasing in η_1; therefore $\partial h_2^*/\partial\eta_1 > 0$.

Proof. We can follow the same strategy as in the case of proving $\partial h_1^*/\partial \eta_2 > 0$. Starting from (6.17d), we get

$$-(h_2^*)^{-2}\,\frac{\partial h_2^*}{\partial \eta_1} - A(1-\eta_2-\frac{\gamma}{2})(\eta_2+\frac{\gamma}{2})\,\theta_2^* u_2^* (h_1^*)^{\frac{\gamma}{2}} (h_2^*)^{\eta_2+\frac{\gamma}{2}-2}\,\frac{\partial h_2^*}{\partial \eta_1}$$

$$-A(1-\frac{\gamma}{2})\frac{\gamma}{2}\,\theta_1^* u_1^* (h_1^*)^{\eta_1+\gamma} (h_2^*)^{\frac{\gamma}{2}-2}\,\frac{\partial h_2^*}{\partial \eta_1} + A\frac{\gamma}{2}\,\theta_1^* u_1^* (h_1^*)^{\eta_1+\frac{\gamma}{2}} (h_2^*)^{\frac{\gamma}{2}-1}\ln(h_1^*) = 0,$$

which, like previously, is the sum of four terms, including three coefficients multiplying $\partial h_2^*/\partial \eta_1$. Under the stated assumptions $\gamma > 0$ and $0.5 > \eta_i + \gamma/2 > 0$, and given the results $h_i^* > 0$, $\theta_i^* > 0$ and $u_i^* > 0$ for $i = 1, 2$, all three coefficients on $\partial h_2^*/\partial \eta_1$ are negative, while the fourth term is positive. Rearranging the equation yields $\partial h_2^*/\partial \eta_1 > 0$. □

Proposition 12: The unique optimum capital stock h_1^* as determined by $h(h_1^*)$ in (6.20) is an increasing function of η_1; therefore $\partial h_1^*/\partial \eta_1 > 0$.

Proof. By direct differentiation, the exponent on h_1^* in (6.20) is decreasing in η_1. Therefore, we only need to show that the multiplier in (6.20) is also decreasing in η_1. The differential of the multiplier with respect to η_1 is negative if the inequality

$$\frac{c\delta^3\gamma^2\left[(\rho+\delta(1-\eta_1))/(\rho+\delta(1-\eta_2))\right]^{\gamma/2(\eta_2-1)}}{4A^2(\eta_2-1)[\rho+\delta(1-\eta_1)]}$$
$$< \frac{c\delta^2\left[(\rho+\delta(1-\eta_1))/(\rho+\delta(1-\eta_2))\right]^{\gamma/2(\eta_2-1)}(2\eta_2+\gamma-2)[2\rho+\delta(2-2\eta_2-\gamma)]}{4A^2(\eta_2-1)[\rho+\delta(1-\eta_2)]}$$

holds. Proceeding by assuming the inequality holds and simplifying leads to

$$\frac{\delta\gamma^2}{\rho+\delta(1-\eta_1)} > \frac{(2\eta_2+\gamma-2)[2\rho+\delta(2-2\eta_2-\gamma)]}{\rho+\delta(1-\eta_2)}.$$

Under the parameter restrictions $2\eta_2+\gamma-2<0$, the right-hand side is thus negative while the left-hand side is positive; therefore the inequality holds and $\dfrac{\partial h_1^*}{\partial \eta_1} > 0$. □

Proposition 13: The unique optimum capital stock h_2^* as determined by $h(h_1^*)$ in (6.20) and the term in (6.19) is an increasing function of η_2; therefore $\partial h_2^*/\partial \eta_2 > 0$.

Proof. It has already been demonstrated that $\partial h_1^*/\partial \eta_2 > 0$. The exponent on h_1^* in (6.19) is also increasing in η_2. As $h_1^* > 1$, the term

$$(h_1^*)^{(1-\eta_1)/(1-\eta_2)}$$

is increasing in η_2. Now we only need to show that the multiplier in (6.19) is also increasing in η_2. The differential of the multiplier with respect to η_2 is positive if

$$\frac{\ln\big[(\rho+\delta(1-\eta_1))/(\rho+\delta(1-\eta_2))\big]+1}{2\big[(\rho+\delta(1-\eta_1))/(\rho+\delta(1-\eta_2))\big]^{1/2(\eta_2-1)}(\eta_2-1)^2} > \frac{\rho}{2[\rho+\delta(1-\eta_2)]\big[(\rho+\delta(1-\eta_1))/(\rho+\delta(1-\eta_2))\big]^{1/2(\eta_2-1)}(\eta_2-1)^2},$$

which implies the inequality

$$\ln\Big[\frac{\rho+\delta(1-\eta_1)}{\rho+\delta(1-\eta_2)}\Big] > \frac{\rho}{\rho+\delta(1-\eta_2)} - 1.$$

This certainly holds if the infimum of the left-hand side expression is greater than the supremum of the right-hand side expression. By monotonicity of the outer function on the left, the infimum occurs where the numerator has its infimum (at $\eta_1 = 0.5$) and the denominator has its supremum (at $\eta_2 = 0$). Consequently, the infimum of the left-hand side expression is

$$\ln\Big[\frac{\rho+\delta/2}{\rho+\delta}\Big].$$

To find the supremum of the right-hand side expression, note that the expression is increasing in η_2, so its supremum is

$$-\frac{\delta/2}{\rho+\delta/2},$$

attained at $\eta_2 = 0.5$. Consequently, $\partial h_2^*/\partial\eta_2 > 0$ since the inequality

$$\ln\Big[\frac{\rho+\delta/2}{\rho+\delta}\Big] + \frac{\delta}{2\rho+\delta} > 0$$

holds as pointed out in the case of $\partial h_1^*/\partial\eta_2 > 0$. □

Appendix K

Proposition 14: The Hessian $\tilde{H}$ of $\tilde{J}^*(\beta)$ is indefinite.

Proof. We must take into account that $\tilde{H}$, containing the second partial derivatives of $\tilde{J}^*(\beta)$ with respect to the parameters A, η_1 and η_2, is symmetric. Therefore it can be written in the form

$$\tilde{H} = \begin{bmatrix} 0 & a & b \\ a & c & 0 \\ b & 0 & d \end{bmatrix},$$

with all nonzero elements a, b, c, d strictly positive and real. Hence

$$|\tilde{H}| = -a^2 d - b^2 c < 0.$$

Since the determinant equals the product of the eigenvalues, the negative determinant implies that $\tilde{H}$ is indefinite (one eigenvalue negative while the other two are positive) or negative definite (all three eigenvalues negative). For a matrix to be negative definite, Sylvester's alternating sign condition must hold (Horn and Johnson, 2013, pp. 430-439), namely

$$(-1)^1 D_1 > 0, \qquad (-1)^2 D_2 > 0, \qquad (-1)^3 D_3 > 0,$$

where $D_1 < 0,\ D_2 > 0,\ D_3 < 0$ are the leading principal minors with alternating signs. In the case of $\tilde{H}$, $D_1 < 0$ certainly does not hold because $D_1 = 0$. Likewise, $D_2 > 0$ does not hold either since $D_2 = -a^2 < 0$. The criterion is conclusive here even though the first leading principal minor that breaks Sylvester's pattern is zero (i.e. $\tilde{H}_{11} = D_1 = 0$). On this ground $\tilde{H}$ might also be negative semidefinite. Negative semidefiniteness, however, is ruled out by the strict negativity of $|\tilde{H}|$. Under negative semidefiniteness at least one eigenvalue would be zero and the determinant would be zero. Therefore $\tilde{H}$ is indefinite. □

References

Barro, R. J. (1974). Are government bonds net wealth? *Journal of Political Economy*, 82(6):1095–1117.

Ben-Porath, Y. (1967). The production of human capital and the life cycle of earnings. *Journal of Political Economy*, 75(4):352–365.

Bertsekas, D. P. (1976). *Dynamic Programming and Stochastic Control*. Academic Press, New York.

Bilstein, R. E. (1980). *Stages to Saturn: A Technological History of the Apollo/Saturn Launch Vehicles*. NASA History Office, Washington, DC.

Borman, G. D., Hewes, G. M., Overman, L. T., and Brown, S. (2003). Comprehensive school reform and achievement: A meta-analysis. *Review of Educational Research*, 73(2):125–230.

Caputo, M. R. (1990a). How to do comparative dynamics on the back of an envelope in optimal control theory. *Journal of Economic Dynamics and Control*, 14(3-4):655–683.

Caputo, M. R. (1990b). A qualitative characterization of the competitive nonrenewable resource extracting firm. *Journal of Environmental Economics and Management*, 18(3):206–226.

Caputo, M. R. (2005). *Foundations of Dynamic Economic Analysis: Optimal Control Theory and Applications*. Cambridge University Press, Cambridge.

Coleman, J. S., Campbell, E. Q., Hobson, C. J., McPartland, J., Mood, A. M., Weinfeld, F. D., and York, R. L. (1966). *Equality of Educational Opportunity*. Office of Education, U.S. Department of Health, Education & Welfare, Washington, DC.

Cunha, F., Heckman, J. J., and Schennach, S. M. (2010). Estimating the technology of cognitive and noncognitive skill formation. *Econometrica*, 78(3):883–931.

Epple, D. and Romano, R. E. (1998). Competition between private and public schools, vouchers, and peer-group effects. *American Economic Review*, 88(1):33–62.

Galbács, P. (2026). Replication Python files for "Rational Drive for School Segregation in a Model of Learning". https://doi.org/10.5281/zenodo.22899304. Zenodo repository.

Gutierrez, S., Whitmer, R. A., Soh, Y., Peterson, R., George, K. M., Lor, Y., and Gilsanz, P. (2024). School-based racial segregation, social support, and late-life cognitive function in the study of healthy aging in african americans (star). *Alzheimer's & Dementia*, 20(9):6257–6267.

Heckman, J. J. (2009). The case for investing in disadvantaged young children. In Lesley, B., editor, *Big Ideas for Children: Investing in Our Nation's Future*, pages 49–58. First Focus, Washington, DC.

Heckman, J. J. and Masterov, D. V. (2007). The productivity argument for investing in young children. *Review of Agricultural Economics*, 29(3):446–493.

Horn, R. A. and Johnson, C. A. (2013). *Matrix Analysis*. Cambridge University Press, Cambridge, UK, 2 edition.

Hoxby, C. M. and Weingarth, G. (2005). Taking race out of the equation: School reassignment and the structure of peer effects. Mimeograph. Retrieved from https://citeseerx.ist.psu.edu/document?repid=rep1&type=pdf&doi=386de4e83235738ec333387e23abf71a4c1f1e4d.

Lucas, R. E. (1988). On the mechanics of economic development. *Journal of Monetary Economics*, 22(1):3–42.

Lucas, R. E. and Moll, B. (2014). Knowledge growth and the allocation of time. *Journal of Political Economy*, 122(1):1–51.

Manski, C. F. (1993). Identification of endogenous social effects: The reflection problem. *Review of Economic Studies*, 60(3):531–542.

Neal, D. A. (2018). *Information, Incentives, and Education Policy*. Harvard University Press, Cambridge, MA.

Oniki, H. (1973). Comparative dynamics (sensitivity analysis) in optimal control theory. *Journal of Economic Theory*, 6(3):265–283.

Orfield, G. and Lee, C. (2007). *Historic Reversals, Accelerating Resegregation, and the Need for New Integration Strategies*. Civil Rights Project/Proyecto Derechos Civiles, UCLA, Los Angeles.

Peterson, R. L., George, K. M., Barnes, L. L., Gilsanz, P., Mayeda, E. R., Glymour, M. M., and Whitmer, R. A. (2021). Association of timing of school desegregation in the united states with late-life cognition in the study of healthy aging in african americans (star) cohort. *JAMA Network Open*, 4(10):1–10.

Sacerdote, B. (2011). Peer effects in education: How might they work, how big are they and how much do we know thus far? In Hanushek, E. A., Machin, S., and Woessmann, L., editors, *Handbook of the Economics of Education*, volume 3, pages 249–277. North Holland, Amsterdam.

Weathers, E. S. and Sosina, V. E. (2022). Separate remains unequal: Contemporary segregation and racial disparities in school district revenue. *American Educational Research Journal*, 59(5):905–938.